

Numerical investigation of surface level instability due to tube in vibrating bed of powder

Yasushi Maeno*

c/o Dr. Y-h. Taguchi, Department of Physics, Tokyo Institute of Technology

Oh-okayama, Meguro-ku, Tokyo 152, Japan

(November 5, 2018)

Abstract

Surface level instability when tube is injected into vibrating bed of powder, which was originally found in experiments, is investigated numerically. We find that thicker (thinner) tube makes surface level inside tube higher (lower) than surface level outside tube. With fixed acceleration amplitude of vibration, surface level inside tube becomes higher as amplitude of vibration increases, which can be explained by considering the dependence upon strength of convective flow.

83.70.Fn, 46.30.Pa, 02.70.Ns, 62.30.+d

Typeset using REVTeX

*All correspondence should be sent to Y-h. Taguchi, at the same address as above. Electronic Address: ytaguchi@cc.titech.ac.jp

I. INTRODUCTION

The dynamics of granular material attracted many attentions of physicists [1]. Among them, vibrating bed of powder was studied by Faraday half and a century ago [2], and many papers were written about its behavior. This is because vibrating bed can exhibit many interesting phenomena like convection [3], surface heaping [5], surface fluidization [6], size segregation [7], and turbulence [8]. Other than those phenomena, surface level instability due to injection of tube into vibrating bed of powder was observed in experiments [9]. The main purpose of this paper is to reproduce this phenomenon numerically.

The organization of this paper is as follows. In Sec. II, we briefly summarized experimental findings by Akiyama and Shimomura. Numerical modeling used in this paper is explained in Sec. III and results will be presented in Sec. IV. Summary and discussion can be found in Sec. V.

II. EXPERIMENTS

Vibrating bed of powder is a vessel filled with granular matter, typically mono-disperse glass beads, and vessel is shaken vertically as strong as gravity acceleration. When acceleration amplitude of vibration exceeds critical value, which is usually a little bit larger than gravity acceleration, the bed exhibits several instabilities, e.g., surface heaping [5], surface fluidization [6], and convection [3]. Further increase of acceleration amplitude results in disappearance of heap, and surface starts to fluctuate violently. In order to measure shear friction in this vibrating bed, Akiyama and Shimomura [9] injected thick tube into vibrating bed and found vary surprising effect. With tube fixed in space, i.e., tube does not vibrate, the surface level inside tube differs from surface level outside tube (Fig. 1), even if heaping is not observed without tube. Thus, this instability may be different from heaping instability observed in vibrating bed. The surface level difference depends upon several physical parameters as diameter of tube, acceleration amplitude, and particle diameter. It was rather

difficult to understand these dependences because experiment of powder can be affected by many other fine differences of conditions, e.g., moisture, temperature, and so on. Thus, numerical investigation is much suitable to understand these dependences in detail.

III. NUMERICAL MODEL

Although there are many numerical schemes for investigating dynamics of powder, we employ here distinct element method (DEM) [10] to reproduce Akiyama's experiments. In DEM, granular particle is modeled as visco-elastic particle, whose interaction is limited within short range. Particularly we employ here non-spherical models introduced by Pöschel and Buchholtz [11], which is known to reproduce static friction effect better than conventional models. In their non-spherical model, each granular particle is modeled as a set of five sub-particles (See Fig. 2). Although tangential force is ignored, static friction can be considered as interaction among surrounding four small sub-particles. Since relative position between center sub-particle and surrounding small sub-particles are considered, rotation of non-spherical particle can be considered effectively. Each sub-particle obeys the following equation

$$m_i \frac{d^2 \vec{r}_i}{dt^2} = \sum_j \vec{F}_{inner}^{ij} + \sum_j \vec{F}_{outer}^{ij} \times \Theta(\ell'_{ij} - |\vec{r}_j - \vec{r}_i|) \quad (1)$$

where F_{inner}^{ij} and F_{outer}^{ij} are interaction within a non-spherical particle and interaction between non-spherical particles respectively. Here subscript i is c or r depending upon whether i sub-particle is center (c) sub-particle or surrounding (r) sub-particle. m_i is mass of i sub-particle and \vec{r}_i is position vector of i sub-particle. Θ is step function, and ℓ'_{ij} is distance between sub-particles which belong to different non-spherical particles,

$$\ell'_{ij} = \begin{cases} 2R_r & (i, j = r, r) \\ 2R_c & (i, j = c, c) \\ R_c + R_r & (i, j = c, r) \end{cases} \quad (2)$$

where R_i is radius of i sub-particle. \vec{F}_{inner}^{ij} is defined as,

$$\vec{F}_{inner}^{ij} = \left[-k(|\vec{r}_i - \vec{r}_j| - \ell_{ij}) - \gamma \left(\frac{d\vec{r}_j}{dt} - \frac{d\vec{r}_i}{dt} \right) \cdot \vec{n}_{ij} \right] \vec{n}_{ij} \quad (3)$$

with $\vec{n}_{ij} \equiv (\vec{r}_j - \vec{r}_i) / |\vec{r}_j - \vec{r}_i|$. k and γ are elastic and viscosity constant respectively, which are related to coefficient of restitution, $e = \exp\left(-\frac{\pi\gamma}{2\sqrt{k-(\gamma/2)^2}}\right)$. ℓ_{ij} is distance between sub-particles among a non-spherical particle,

$$\ell_{ij} = \begin{cases} R_c + R_r & (i, j = c, r) \\ \sqrt{2}(R_c + R_r) & (i, j = r, r) \end{cases} \quad (4)$$

This means that five sub-particles have interaction only when their relative positions deviate from that shown in Fig.2. \vec{F}_{outer}^{ij} is defined as

$$\vec{F}_{outer}^{ij} = \left[-k(|\vec{r}_i - \vec{r}_j| - \ell'_{ij}) - \gamma \left(\frac{d\vec{r}_j}{dt} - \frac{d\vec{r}_i}{dt} \right) \cdot \vec{n}_{ij} \right] \vec{n}_{ij} \quad (5)$$

In order to simulate vibrating bed of powder, we have to introduce vessel composed of sub-particles. Interaction between sub-particles which construct non-spherical particles and sub-particles which construct vessels employs the same functional form as \vec{F}_{outer}^{ij} , but ℓ'_{ij} is replaced with

$$\ell'_{ij} = \begin{cases} R_c + R_v & (i, j = c, v) \\ R_r + R_v & (i, j = r, v) \end{cases} \quad (6)$$

Motion of sub-particles which construct vessel is not affected by the interaction with sub-particles which constructs non-spherical particle, but follows given motion of vessel itself, e.g., vibration or static state. In addition to this, 'solid plate' is added to the bottom to prevent particles from falling out of the vessel through bottom. This plate causes vertical force applied to i th sub-particle,

$$F_{bottom}^i = k'[z_{bottom} - z_i], \quad (7)$$

where z_{bottom} and z_i are vertical components of bottom and i th sub-particle, respectively.

IV. THE RESULTS

In the simulations, we employ following parameters (See Fig.3). Radius of sub-particles are $R_c = 3.0$, $R_r = 0.5$, and $R_v = 1.5$. We ignore distribution of radius and use identical non-spherical particles. Number of non-spherical particles are 200, this means, number of sub-particles is 1000. Interaction parameters are taken as $k/m_i = 600.0$ and $\gamma/m_i = 2.0$ independent of the kind of sub-particles. Thus coefficient of restitution $e = 0.88$. k' is take to be $2k$. For size of vessel, its diameter $D_v = 90$ and its height $H_v = 135$. Tube whose height $H_c = 10.5$ is separated from bottom of vessel by $H_s = 45$. Gravity acceleration is taken to be 9.8.

Control parameters of simulation are the acceleration amplitude of vibration Γ , angular frequency of vibration ω , and diameter of tube, D_c . Here Γ is related with ω as $\Gamma = a\omega^2/g$ where a is amplitude of vibration. The values of these parameters used in simulations are, $\Gamma = 5.0, 6.0$, and 7.0 , $\omega = 3.0, 4.0$, and 5.0 , $D_c = 30, 24$, and 18 . Total length of simulation is over 40 periods.

Figure 4 shows typical snapshot of simulation. In order to measure surface level differences, we define height of surface as follows. For example, surface height inside tube z_i is taken such that number of non-spherical particles above z_i is half as much non-spherical particles as aligned along section of tube. (For detail, see Fig. 5.) The height z_o outside tube is defined in similar way. Then height difference between inside and outside tube $\Delta z = z_i - z_o$. In addition to this, we measure flow of non-spherical particles within vessel following ref. [3], i.e., by dividing vessel into cells as large as non-spherical particle, and flow is defined as number of particle transport between cells per period of vibration.

Figure 6 shows the dependence of Δz upon several parameters, and Figure 7 shows flow patterns and strength for several parameter values.

V. SUMMARY AND DISCUSSION

In this paper, we numerically investigated height difference Δz between inside and outside injected tube. Δz increases as diameter D_c of injected tube increases except for a few cases (See Fig. 6). When accelerated amplitude of vibration Γ and D_c are fixed, Δz decreases as angular frequency of vibration ω increases. Since convection becomes weak as ω increases except for a few cases (See Fig. 6), Δz can be regarded as a function of convection indirectly. These results are schematically shown in Fig.8. Upper row corresponds to larger ω and lower row to smaller. Left column shows the results for smaller D_c and right column shows those for larger. Thus, in upper left case, Δz takes minimum, and in lower right case, Δz takes maximum. Also convection which occurs when ω is small enough is drawn in lower row.

Possible qualitative explanation of these results are as follows. Granular material inside tube is affected by both upward and downward forces. Upward force is due to convection. Convection is upward at the center of vessel, thus it push up granular material inside tube. Difference between upper row and lower row is the difference of strength of convection. Lower row has stronger upward force due to convection, thus surface level inside tube is higher in lower row than in upper row.

Downward force is possibly due to difference of density between inside and outside tube. Generally, fluidized granular matter has smaller density than that of fixed bed. However, granular matter inside tube is hard to flow due to friction with tube, thus density is relatively high. This effect pushes down granular matter into tube. This conjecture explains why thinner tube has lower level of granular matter inside tube. Thinner tube causes higher friction which prevents granular matter from being fluidized, thus heavier granular matter is hard to rise by convection. It is schematically illustrated in Fig.8, where left column has lower level of surface inside tube than right column. This conjecture should be confirmed in future.

VI. ACKNOWLEDGEMENT

The author thanks Dr. Hiraku Nishimori at Ibaraki University for providing his experimental results before publication. Prof. J. Rajchenbach is also acknowledged for helpful discussion. The author also thanks Dr. Y-h. Taguchi for his translating Japanese version of this paper into English and for helpful discussions.

REFERENCES

- [1] For general reviews about powder, see e.g., H. M. Jaeger and S. R. Nagel, *Science* **255**, 1523 (1992); H. Hayakawa, H. Nishimori, S. Sasa, and Y-h. Taguchi, *Jpn. J. Appl. Phys.*, 34 (1995) 397; Y-h. Taguchi, H. Hayakawa, S. Sasa, and H. Nishimori eds., *Dynamics of Powder Systems*, *Int. J. Mod. Phys. B* **7** Nos. 9 & 10 (1993); D. Bideau and A. Hansen eds., *Disorder and Granular Media*, (North-Holland, Amsterdam, 1993); A. Mehta ed., *Granular Matter*, (Springer, Berlin, 1993); C. Thornton ed., *Powders and Grains '93* (A.A.Balkema Publishers, Rotterdam, 1993).
- [2] M. Faraday, *Philos. Trans. R. Soc. London* 52 (1831) 299.
- [3] Y-h. Taguchi, *Phys. Rev. Lett.* 69 (1992) 1367.
- [4] J. A. C. Gallas, H. J. Herrmann, S. Sokolowsky, *Phys. Rev. Lett.* 69 (1992) 1371;
- [5] P. Evesque and J. Rajchenbach, *Phys. Rev. Lett.* 62 (1989) 44; C. Laroche, S. Douady, and S. Fauve, *J. Phys. (France)* 50 (1989) 44.
- [6] P. Evesque, E. Sznatula, and J.-P. Dennis, *Europhys. Lett.* 12 (1990) 623.
- [7] J. B. Knight, H. M. Jaeger, and S. R. Nagel, *Phys. Rev. Lett.* 70 (1993) 3728; J. Duran, J. Rajchenbach, and E. Clement, *Phys. Rev. Lett.* 70 (1993) 2431; A. D. Rosato, F. Prinz, K. J. Stanburg, and R. H. Swendsen, *Phys. Rev. Lett.* 58 (1987) 1038.
- [8] Y-h. Taguchi, *J. Phys. (France) II* 2 (1992) 2103; *Europhys. Lett.* 24 (1993) 203; *Fractals* 1 (1993) 1080; *Physica D* 80 (1995) 61.
- [9] T. Akiyama and T. Shimomura, *Powder Technol.* 66 (1991) 243; *Adv. Powder Technol.* 4 (1993) 129.
- [10] P. A. Cundal and O. D. L. Strack, *Geotechnique* 29-1 (1979) 47.
- [11] T. Pöschel and V. Buchholtz, *Phys. Rev. Lett.* 71 (1993) 3963; V. Buchholtz and T. Pöschel, *Physica A* 202 (1994) 390.

FIGURES

FIG. 1. Schematics of experiment [9]

FIG. 2. Each non-spherical particle composed of five sub-particles

FIG. 3. Schematics of numerical simulation

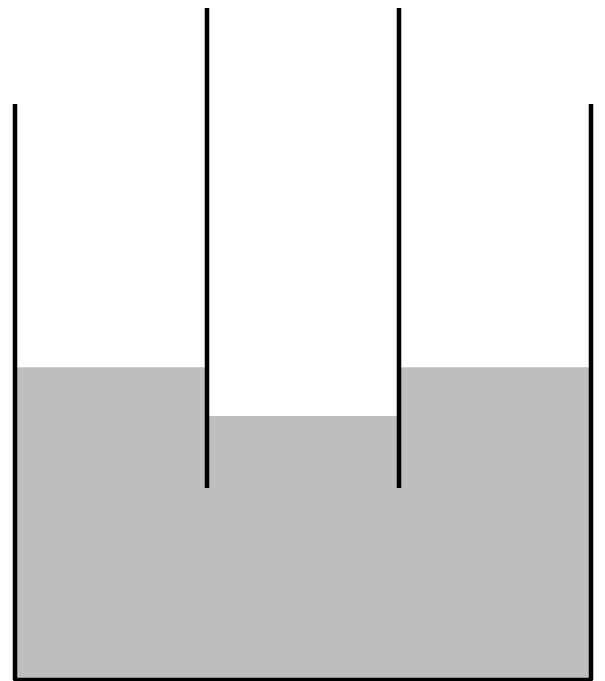
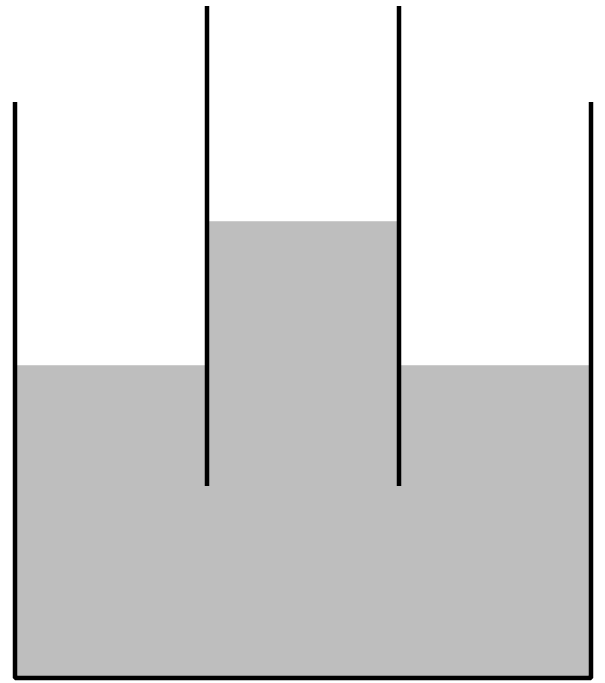
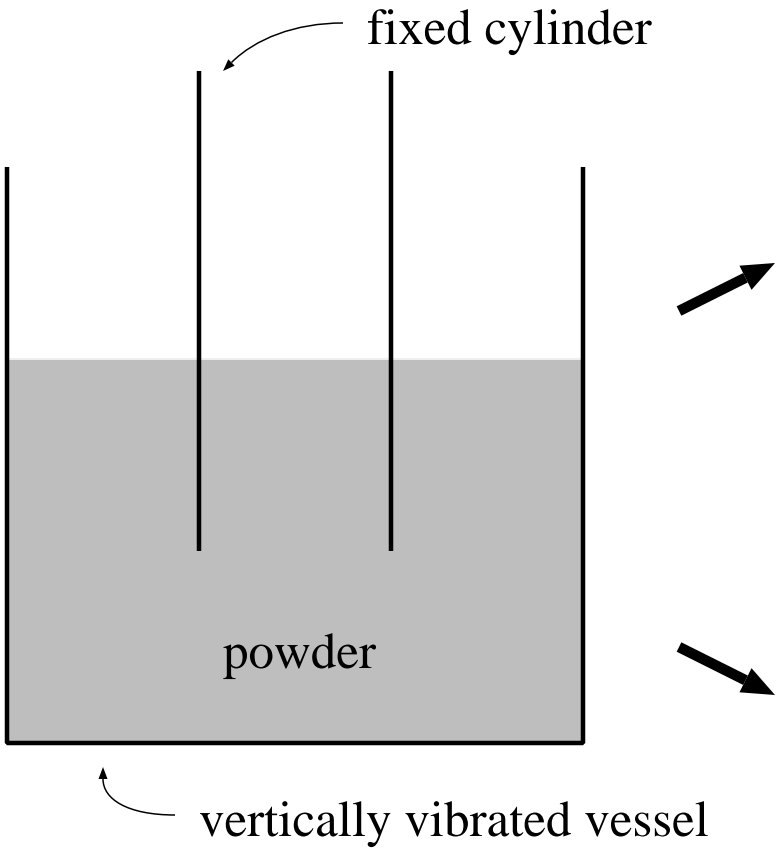
FIG. 4. Snapshot of simulation. Segments attached to each particle reveals instantaneous velocity vectors

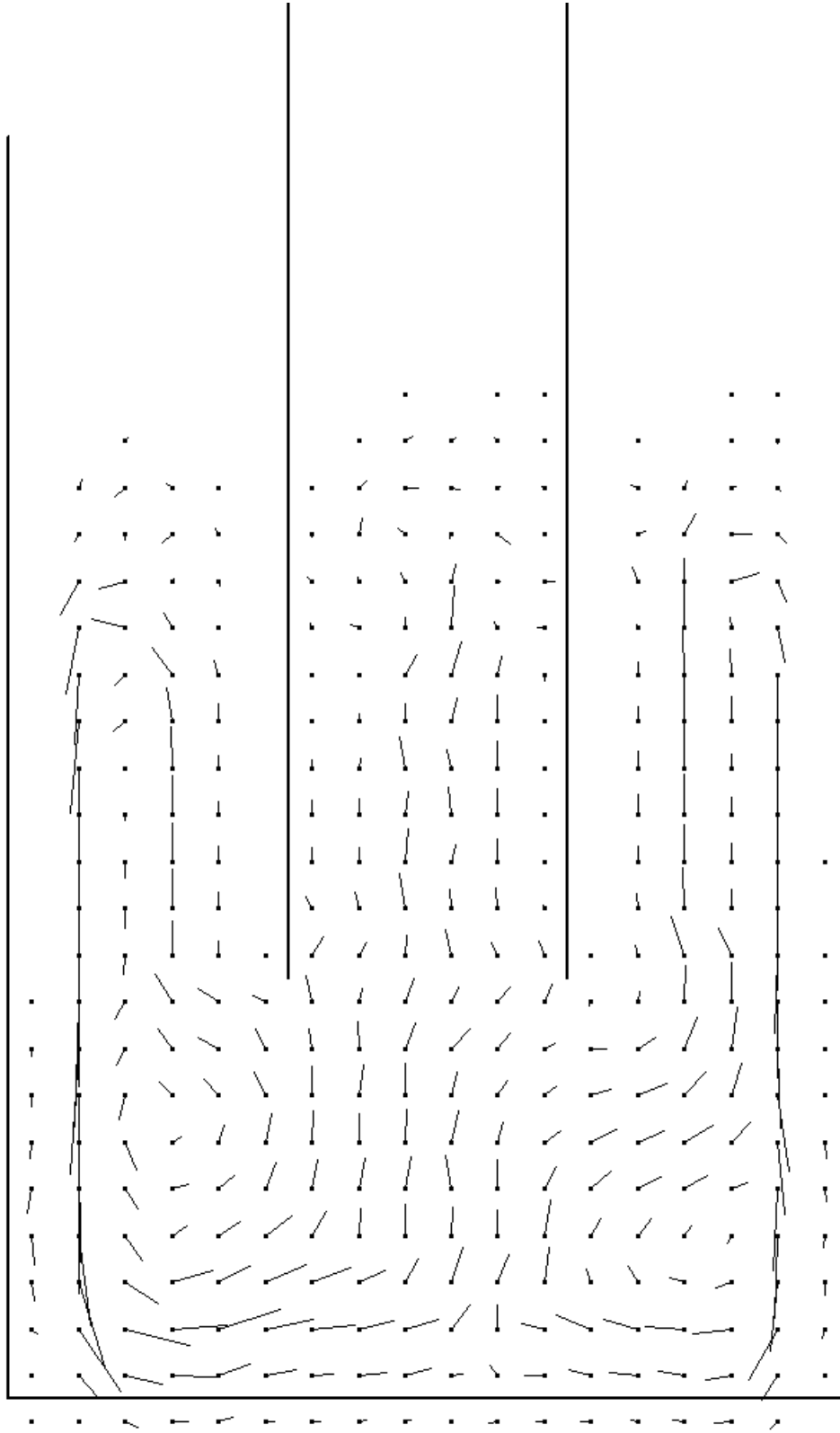
FIG. 5. Definition of height inside tube. $N_i(z)$ is number of non-spherical particles above z . The height z_i inside tube is defined such that $N_i(z) = m_i/2$ where m_i is number of non-spherical particles aligned along section of tube ($m_i = 6$ in this figure).

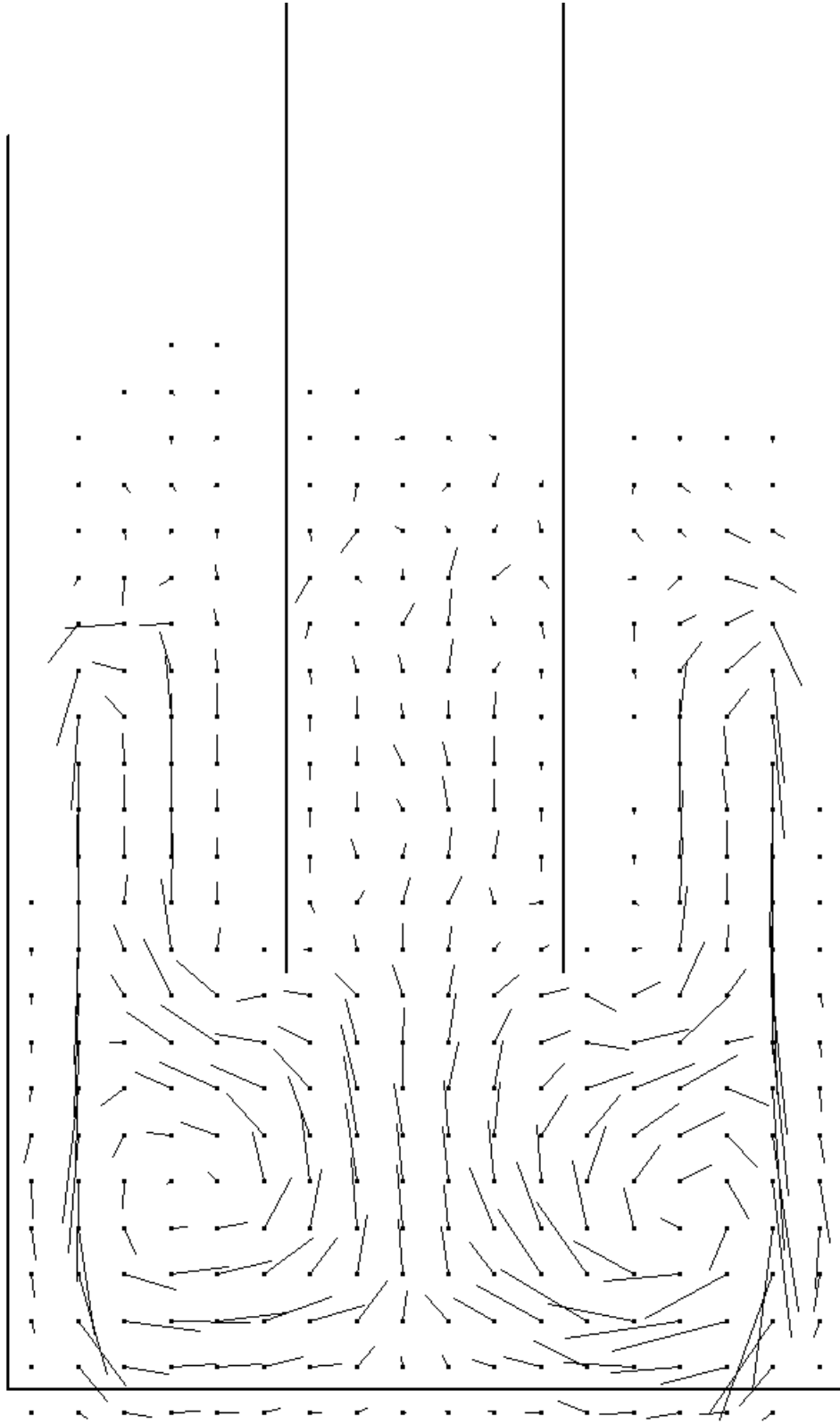
FIG. 6. Δz . $\diamond : \omega = 3.0$, $+: \omega = 4.0$, $\square : \omega = 5.0$. (a) $\Gamma = 5.0$ (b) $\Gamma = 6.0$ (c) $\Gamma = 7.0$

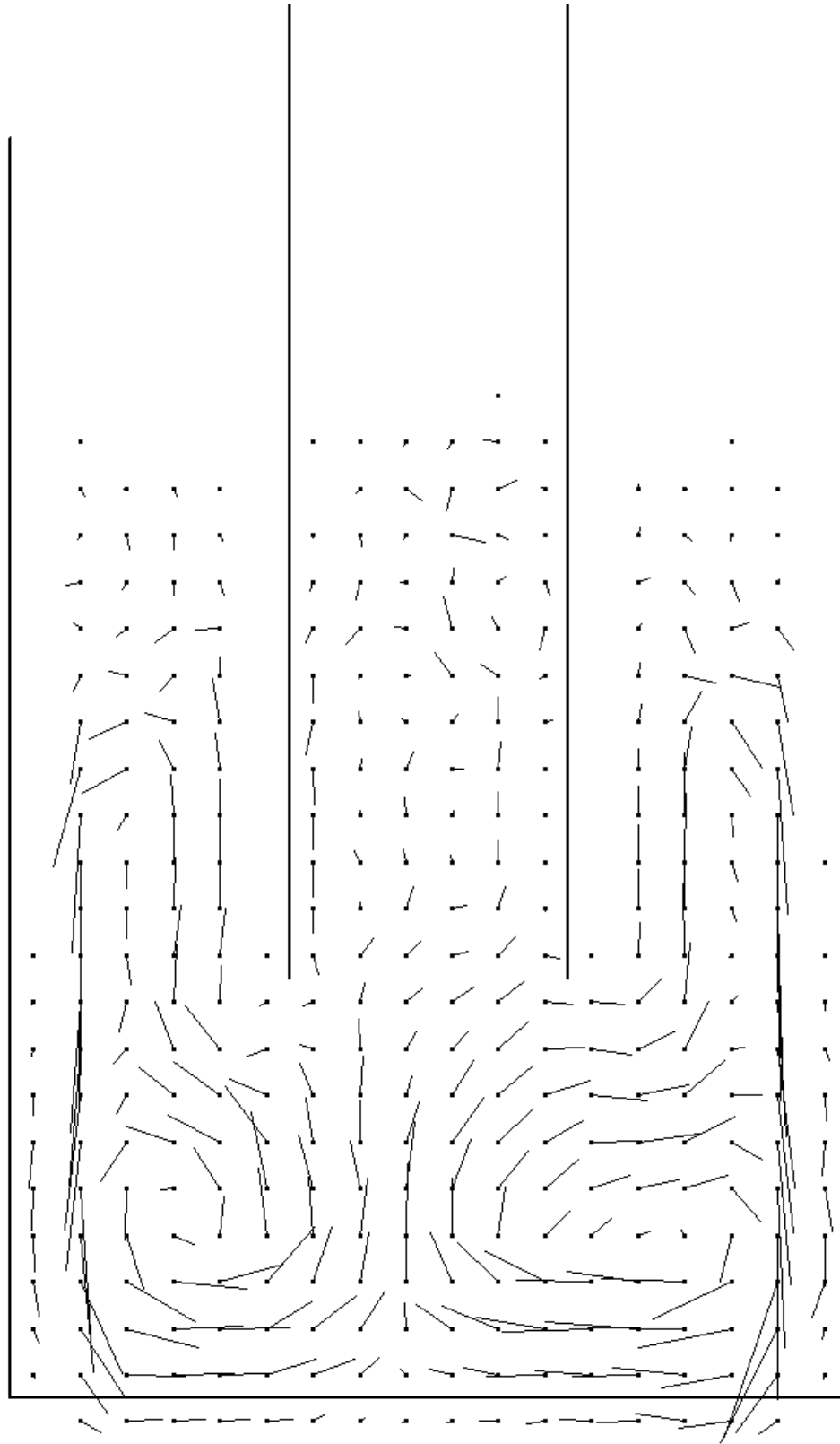
FIG. 7. Flow patterns and its strength (I). (a) $\Gamma = 5.0, \omega = 3.0$. Wide tube: $I = 1302$, middle tube: $I = 1103$, narrow tube: $I = 1891$. (b) $\Gamma = 6.0, \omega = 3.0$. Wide tube: $I = 2821$, middle tube: $I = 2426$, narrow tube: $I = 2546$. (c) $\Gamma = 7.0, \omega = 3.0$. Wide tube: $I = 2800$, middle tube: $I = 2426$, narrow tube: $I = 3409$. (d) $\Gamma = 5.0, \omega = 4.0$. Wide tube: $I = 446$, middle tube: $I = 436$, narrow tube: $I = 433$. (e) $\Gamma = 6.0, \omega = 4.0$. Wide tube: $I = 686$, middle tube: $I = 707$, narrow tube: $I = 554$. (f) $\Gamma = 7.0, \omega = 4.0$. Wide tube: $I = 931$, middle tube: $I = 746$, narrow tube: $I = 551$. (g) $\Gamma = 5.0, \omega = 5.0$. Wide tube: $I = 368$, middle tube: $I = 235$, narrow tube: $I = 212$. (h) $\Gamma = 6.0, \omega = 5.0$. Wide tube: $I = 311$, middle tube: $I = 276$, narrow tube: $I = 289$. (i) $\Gamma = 7.0, \omega = 5.0$. Wide tube: $I = 257$, middle tube: $I = 309$, narrow tube: $I = 233$.

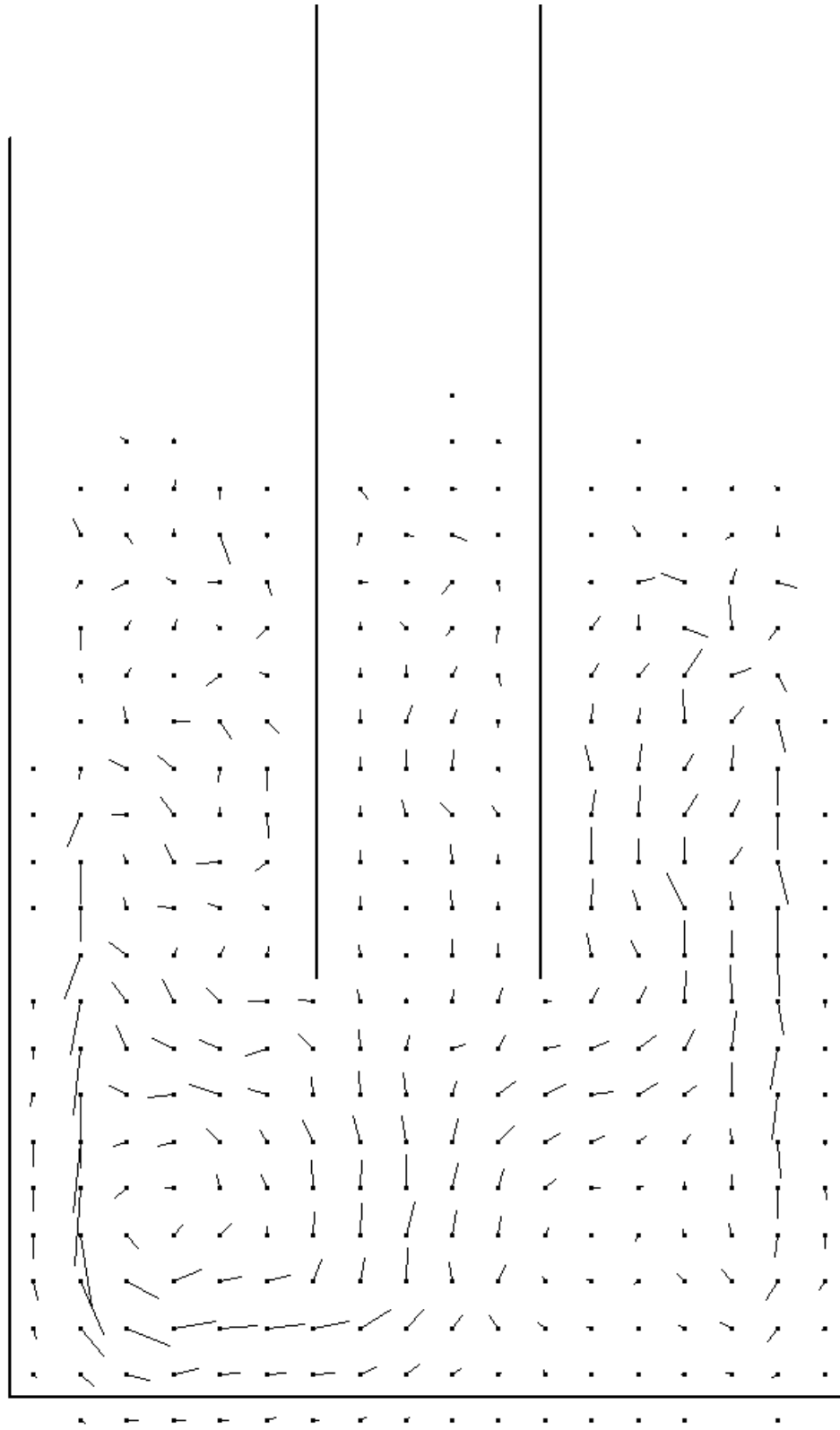
FIG. 8. Schematics of conclusion

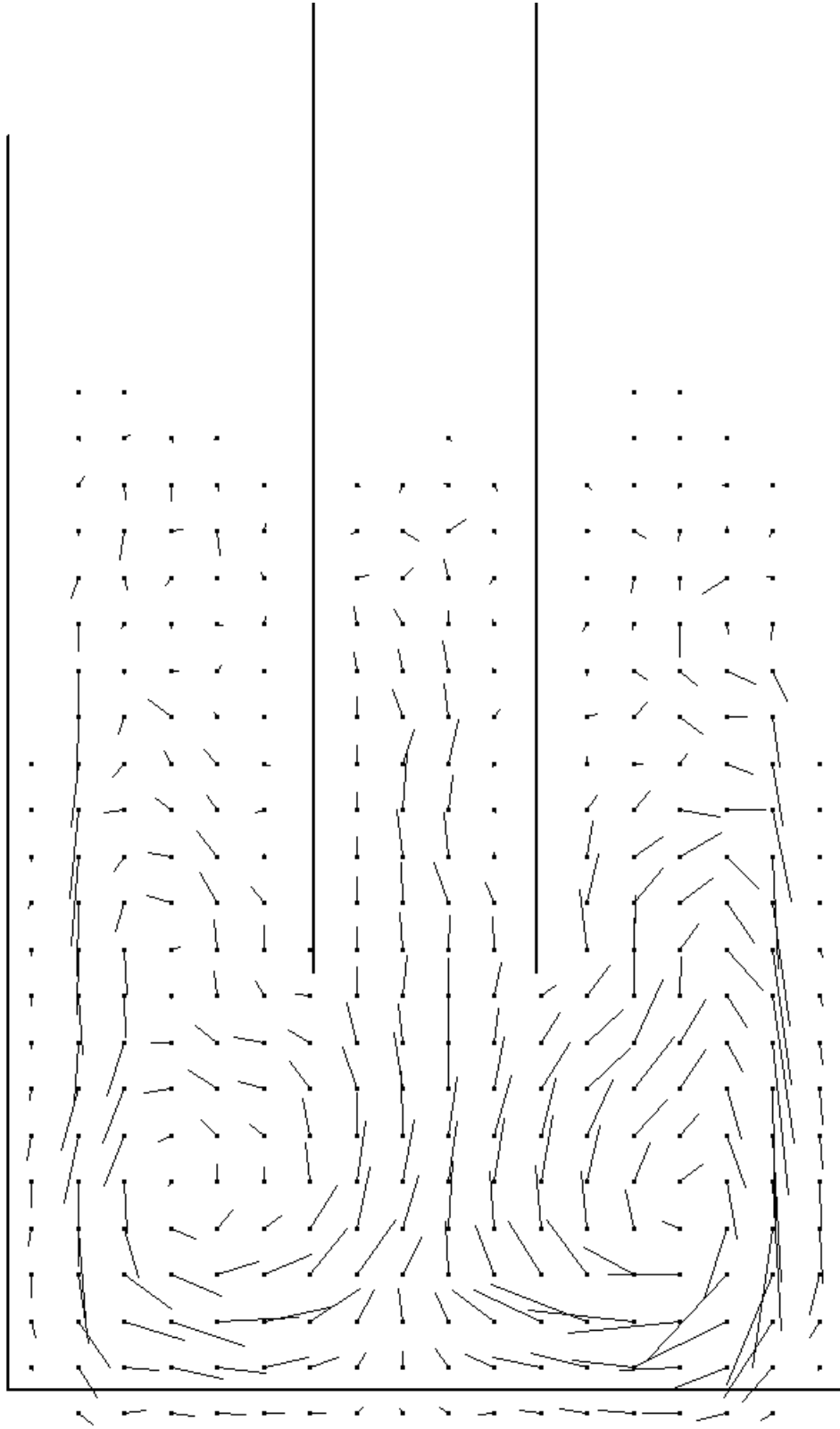


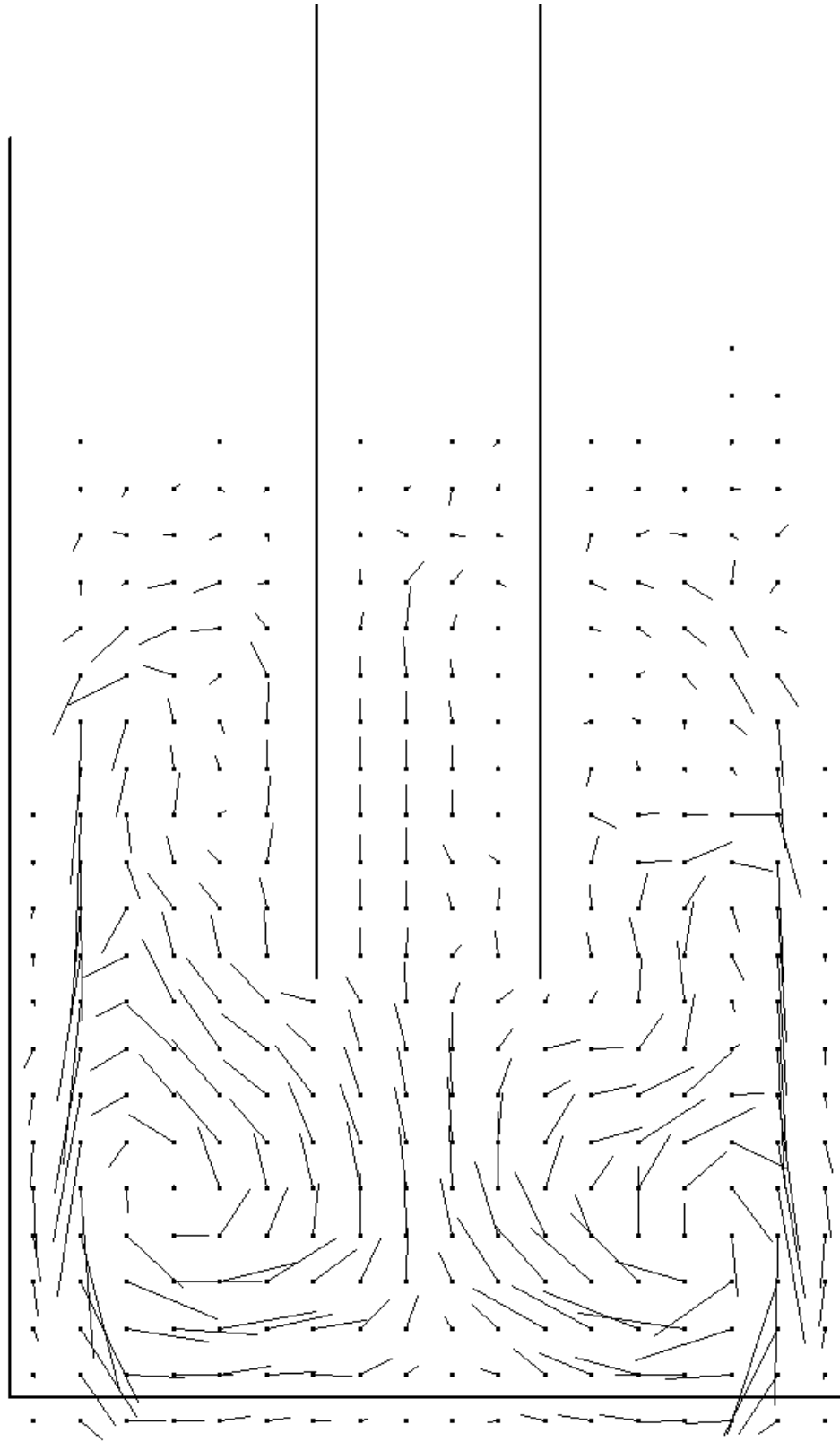


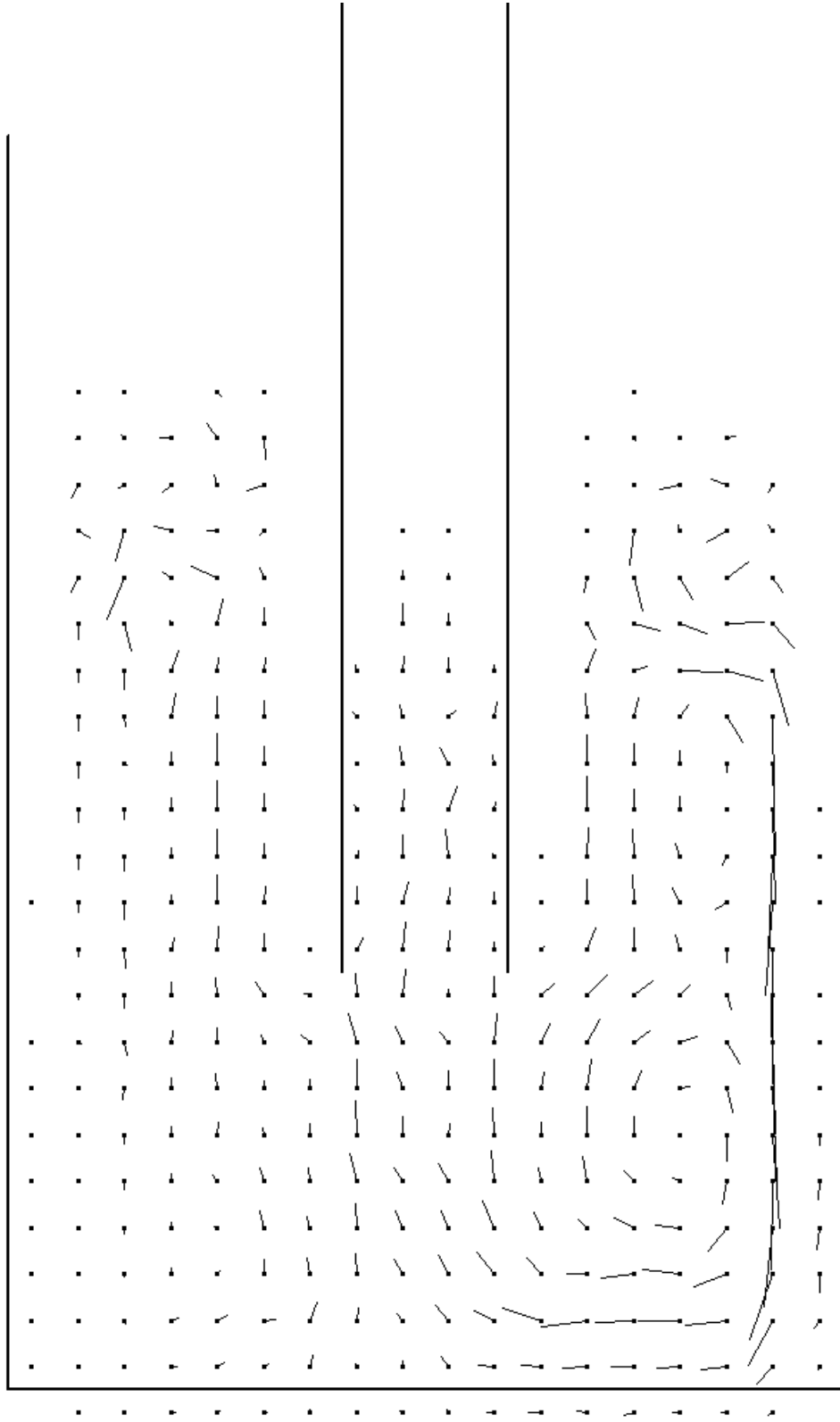


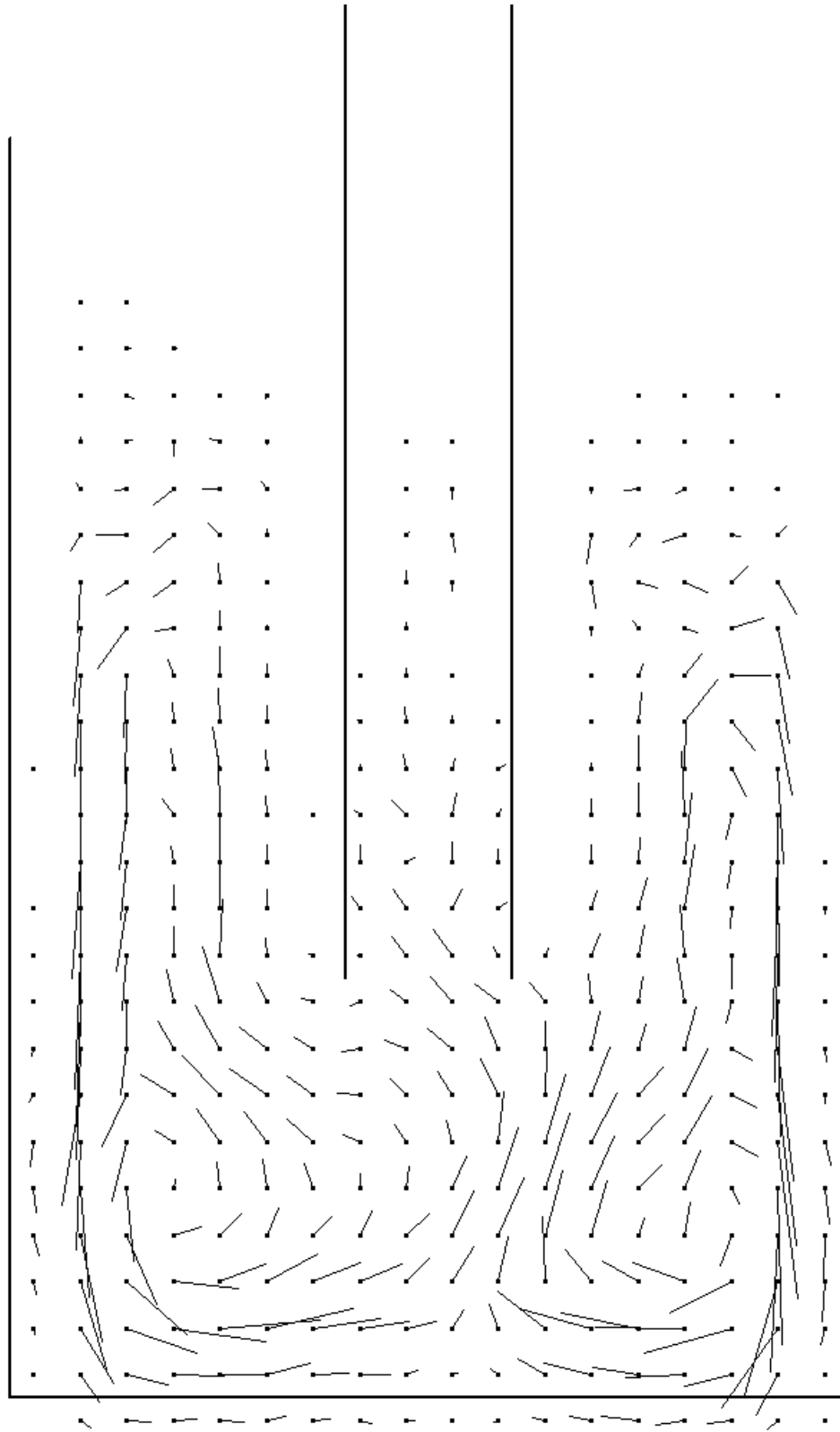


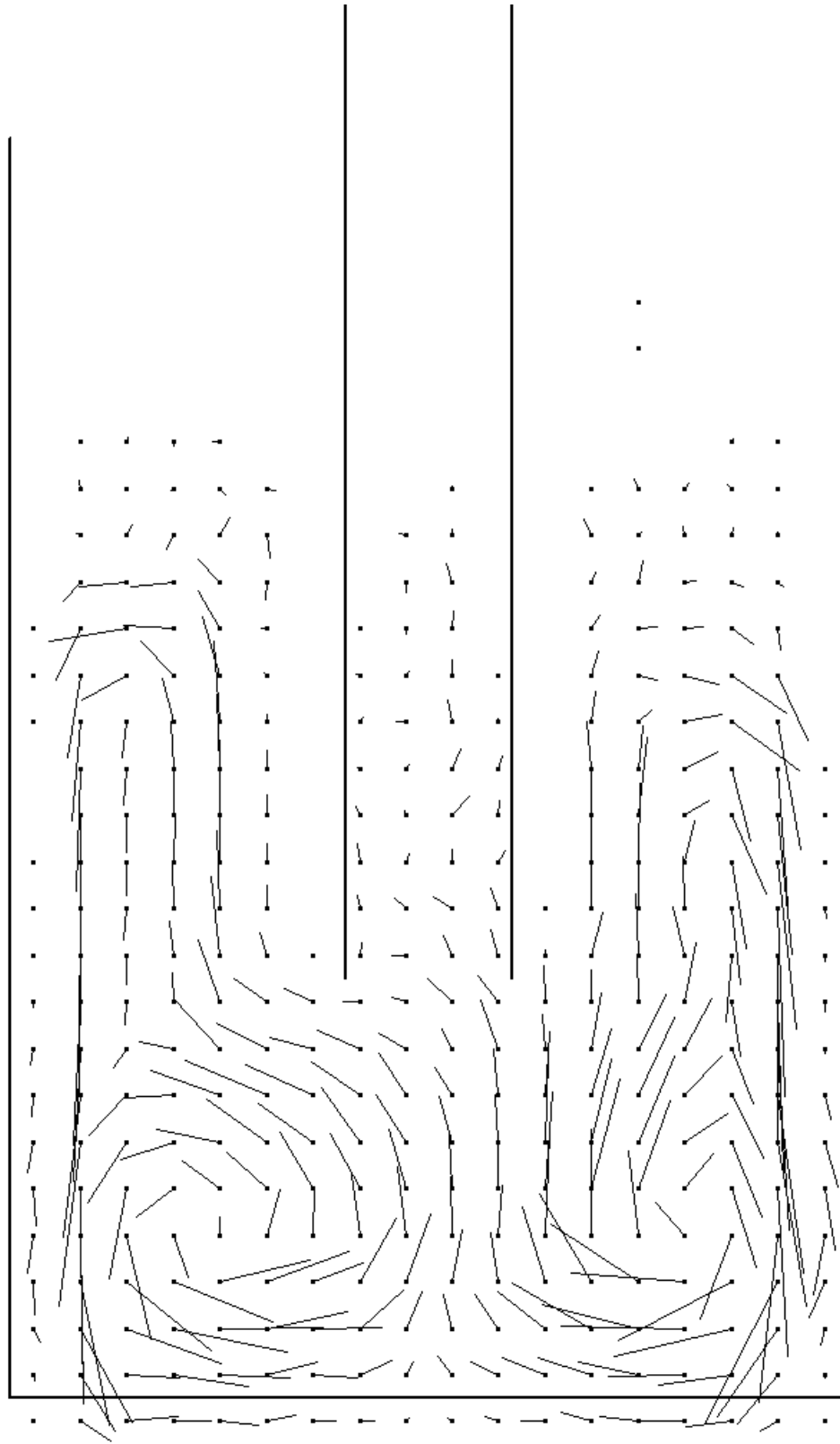


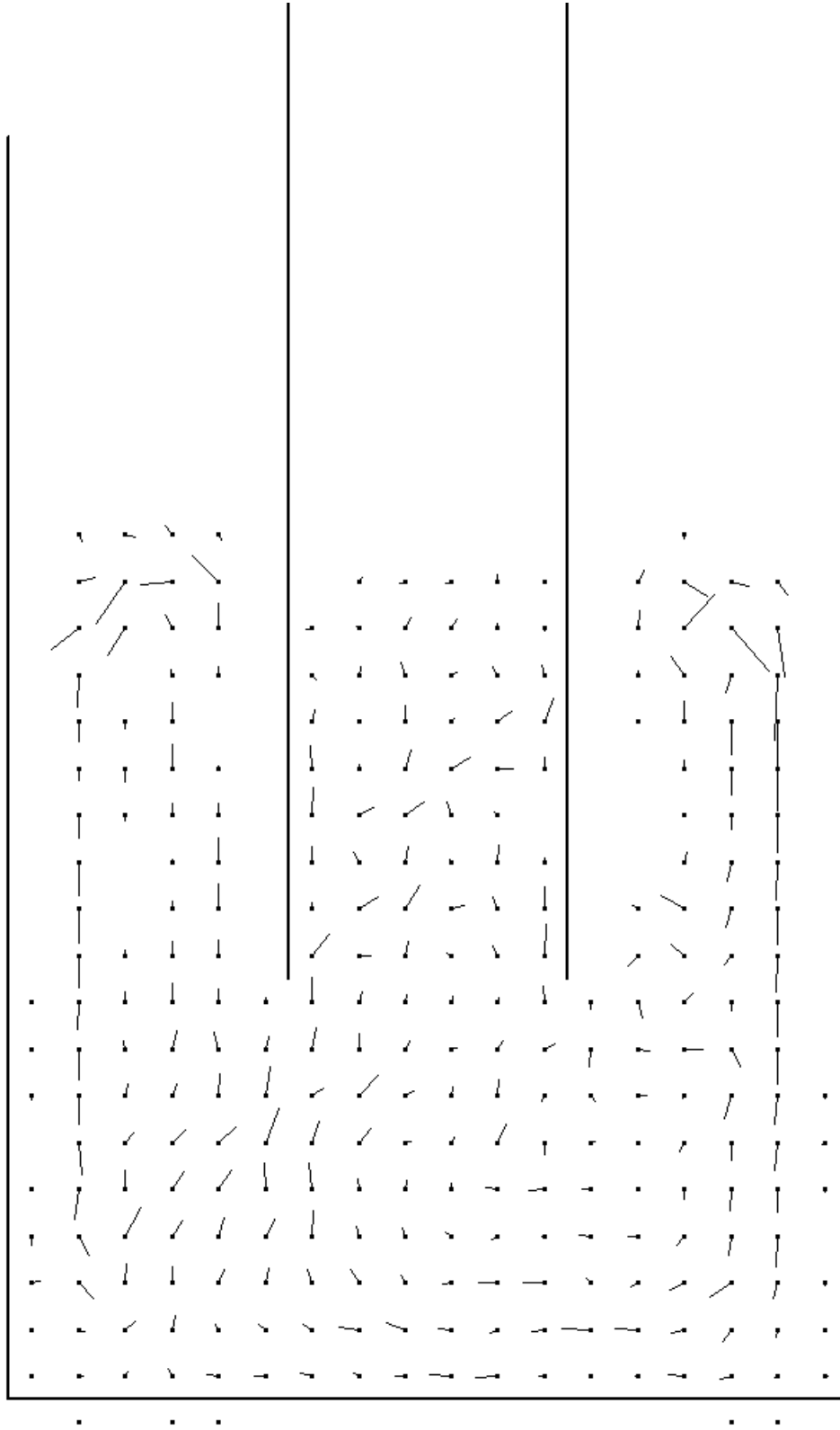


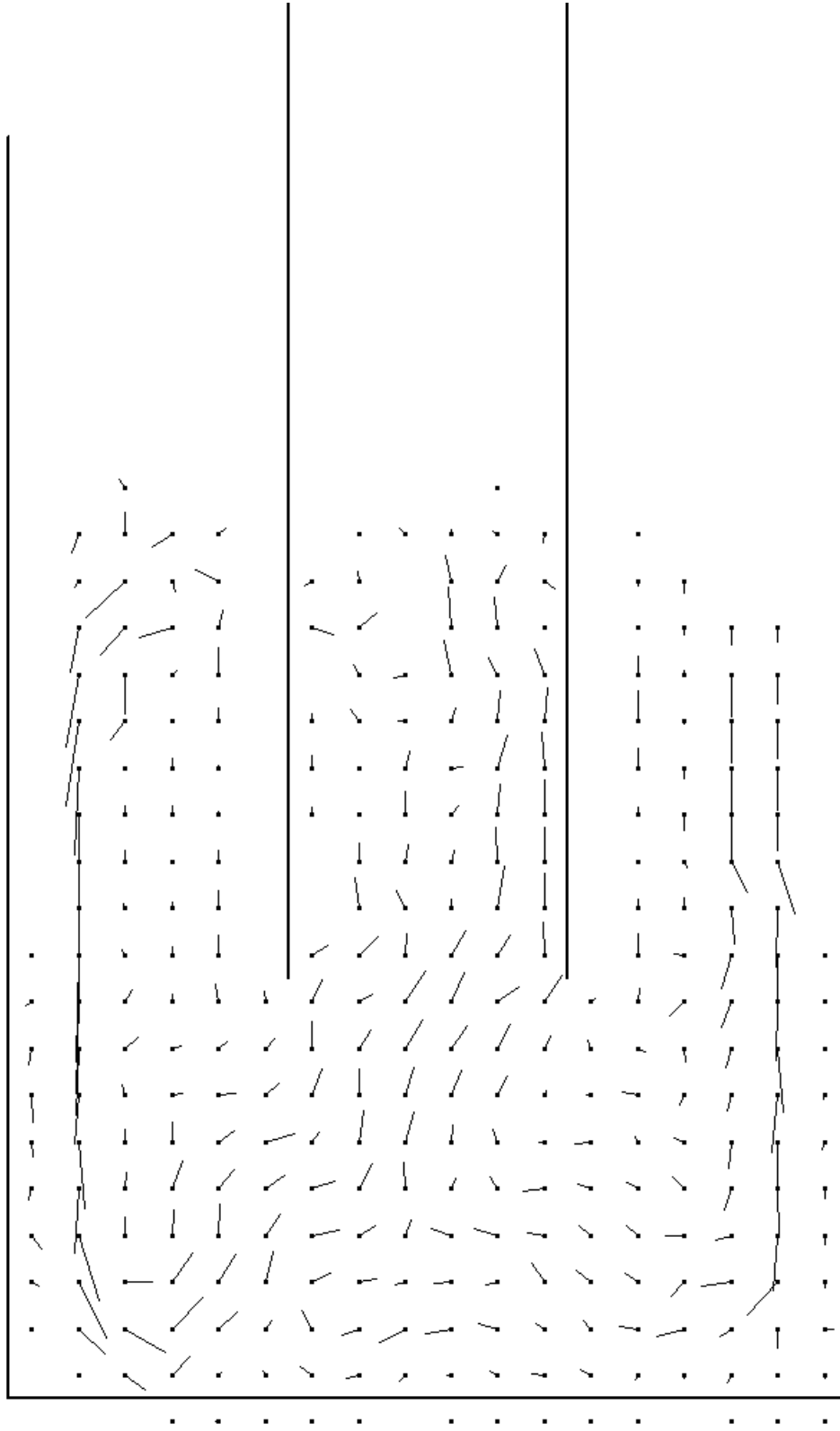


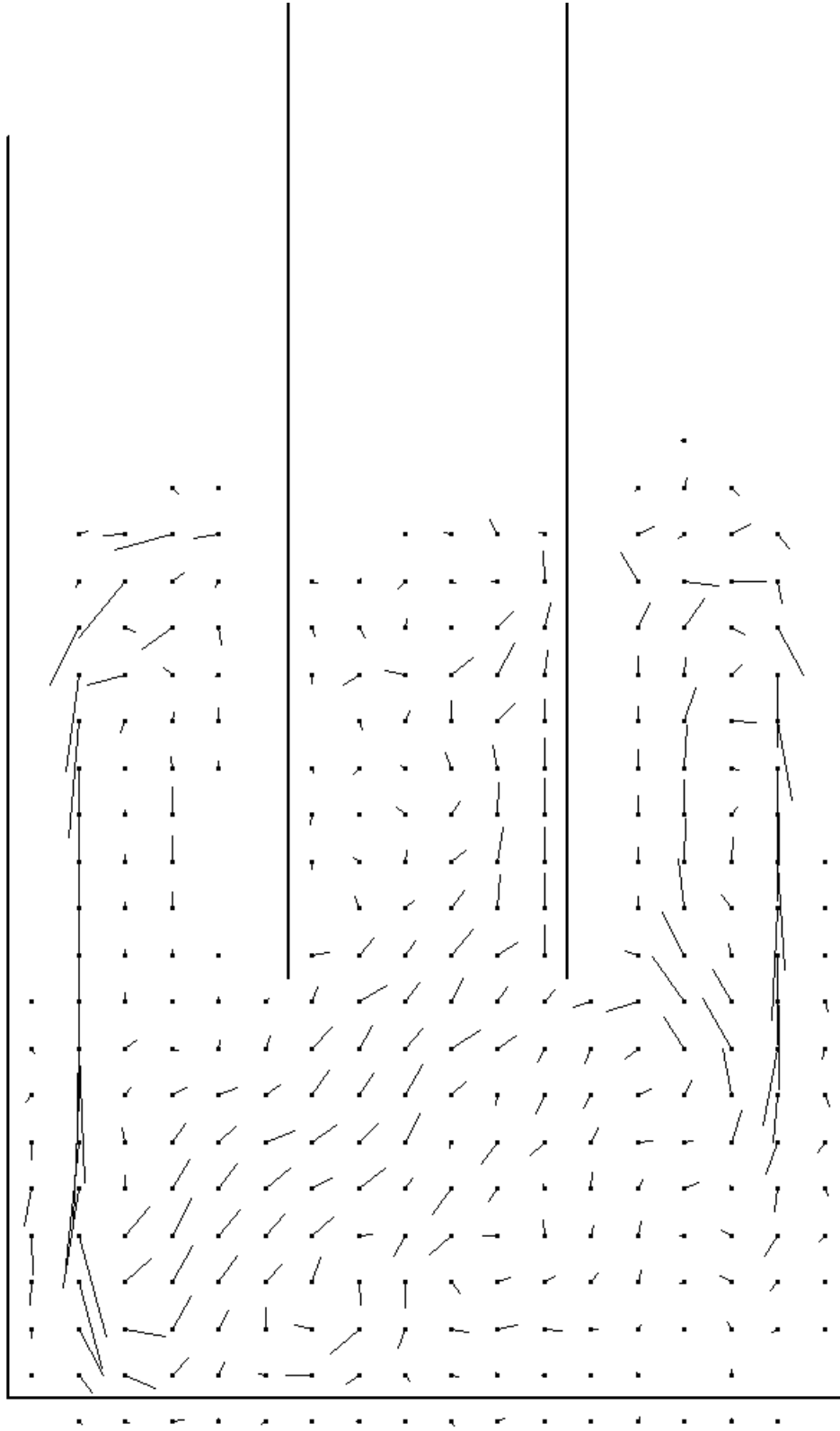


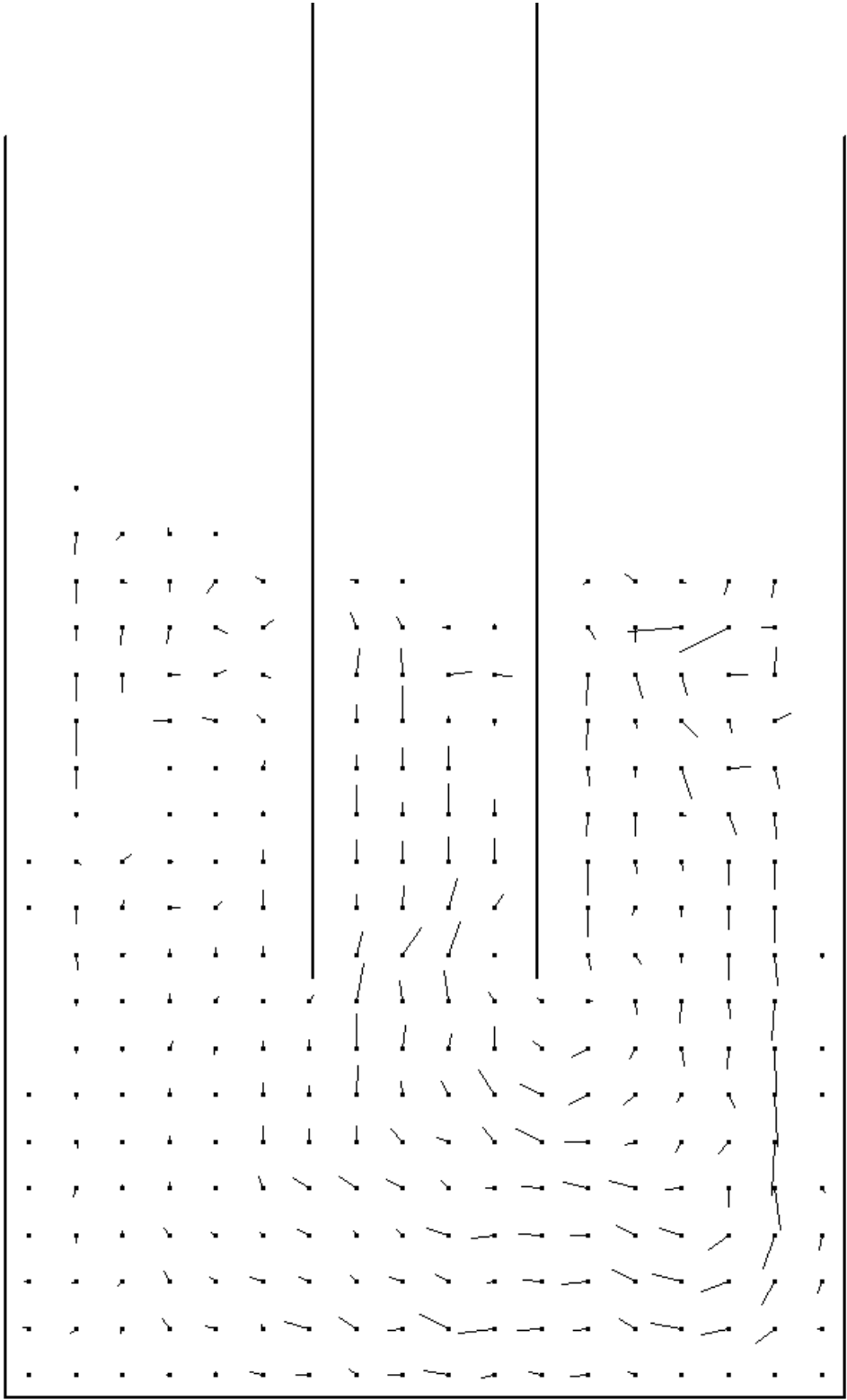


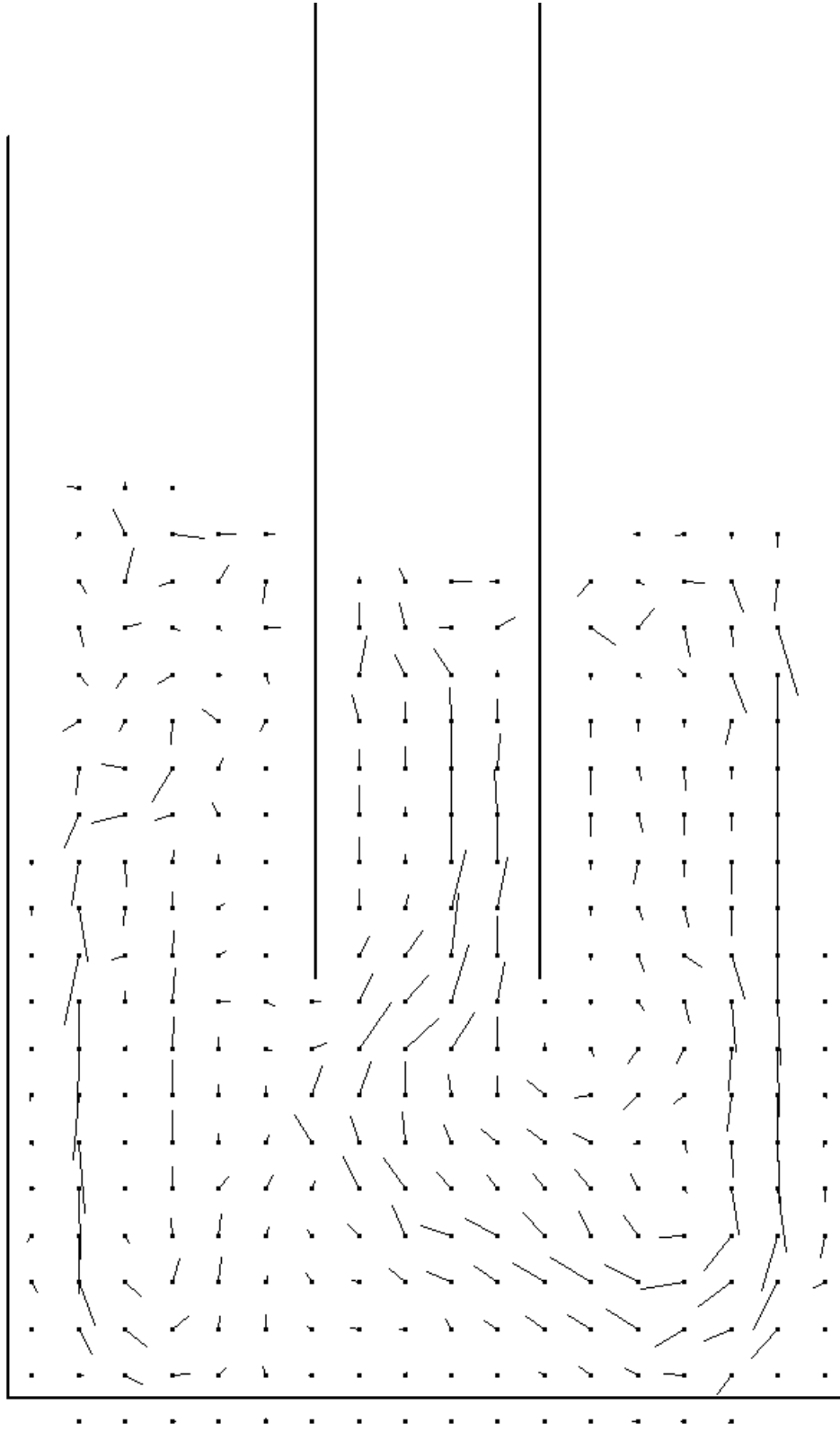


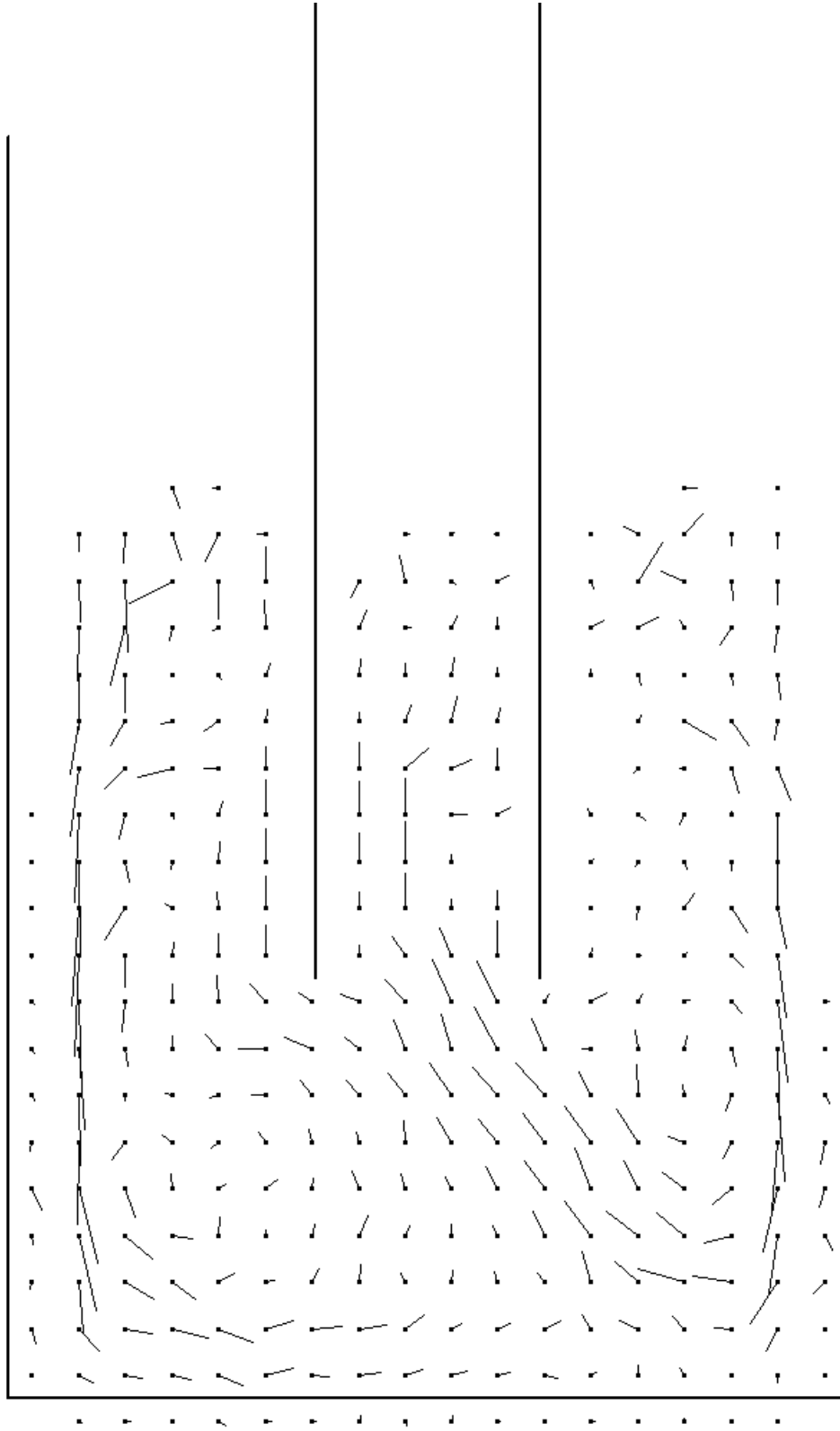


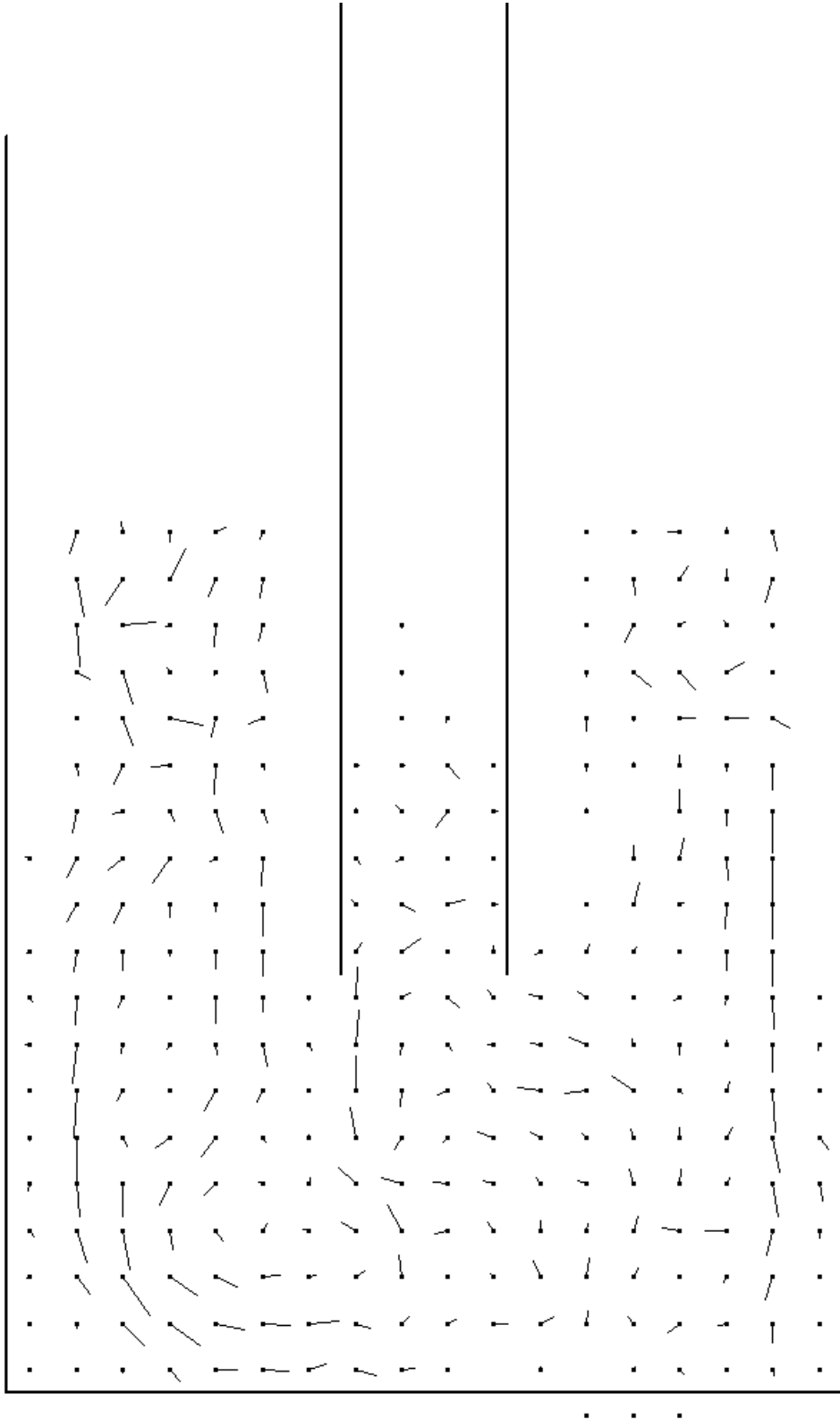




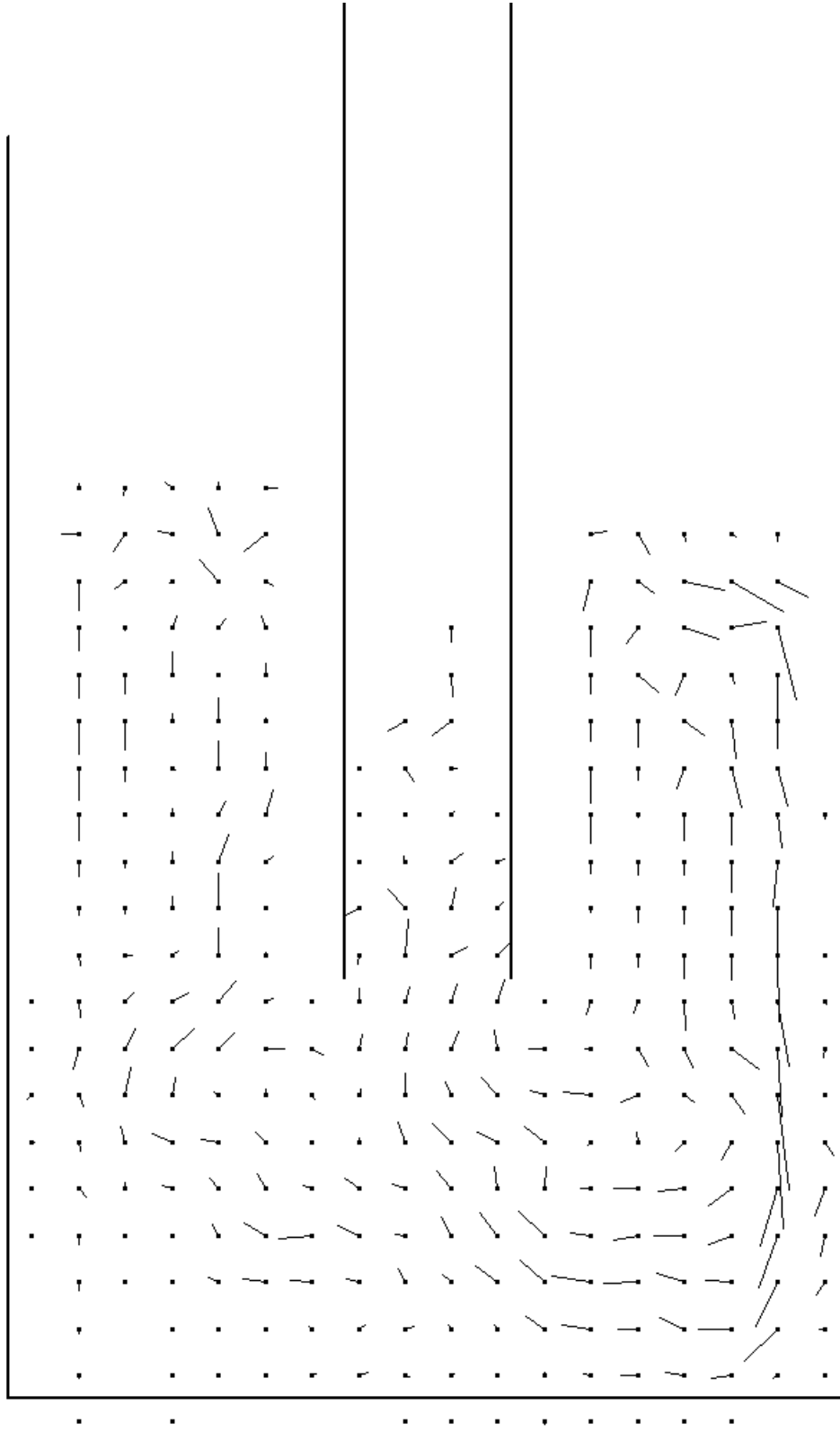


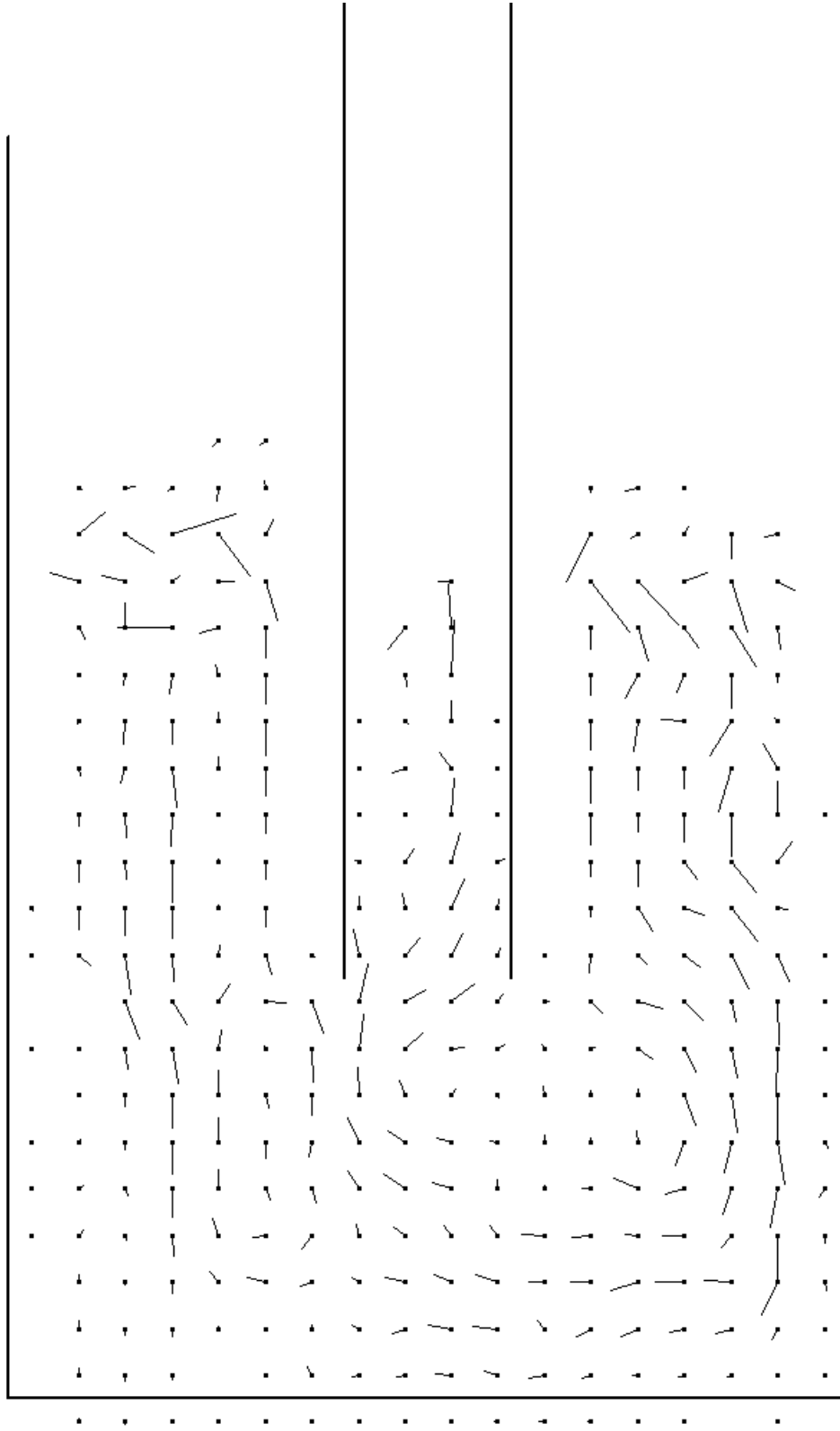


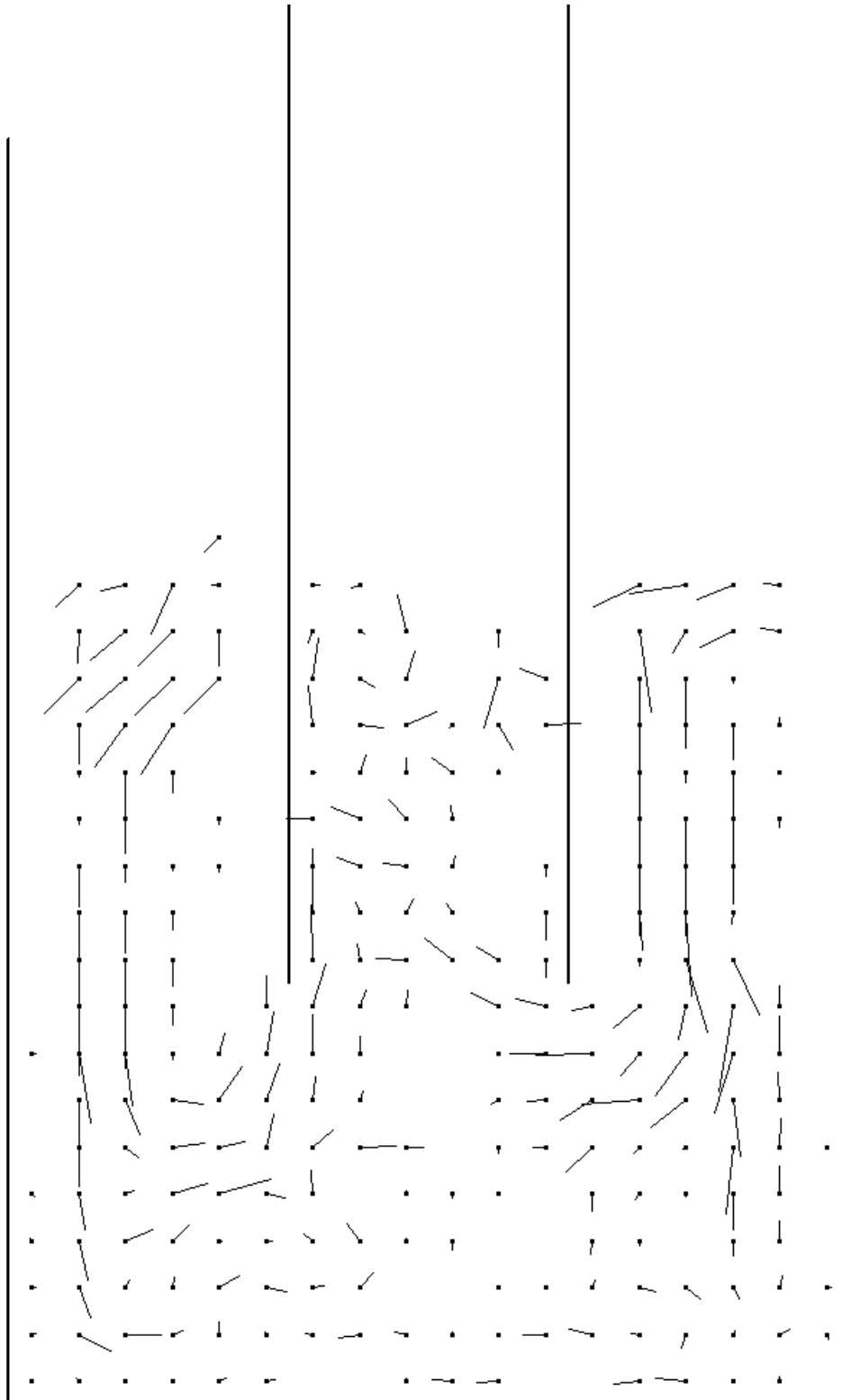


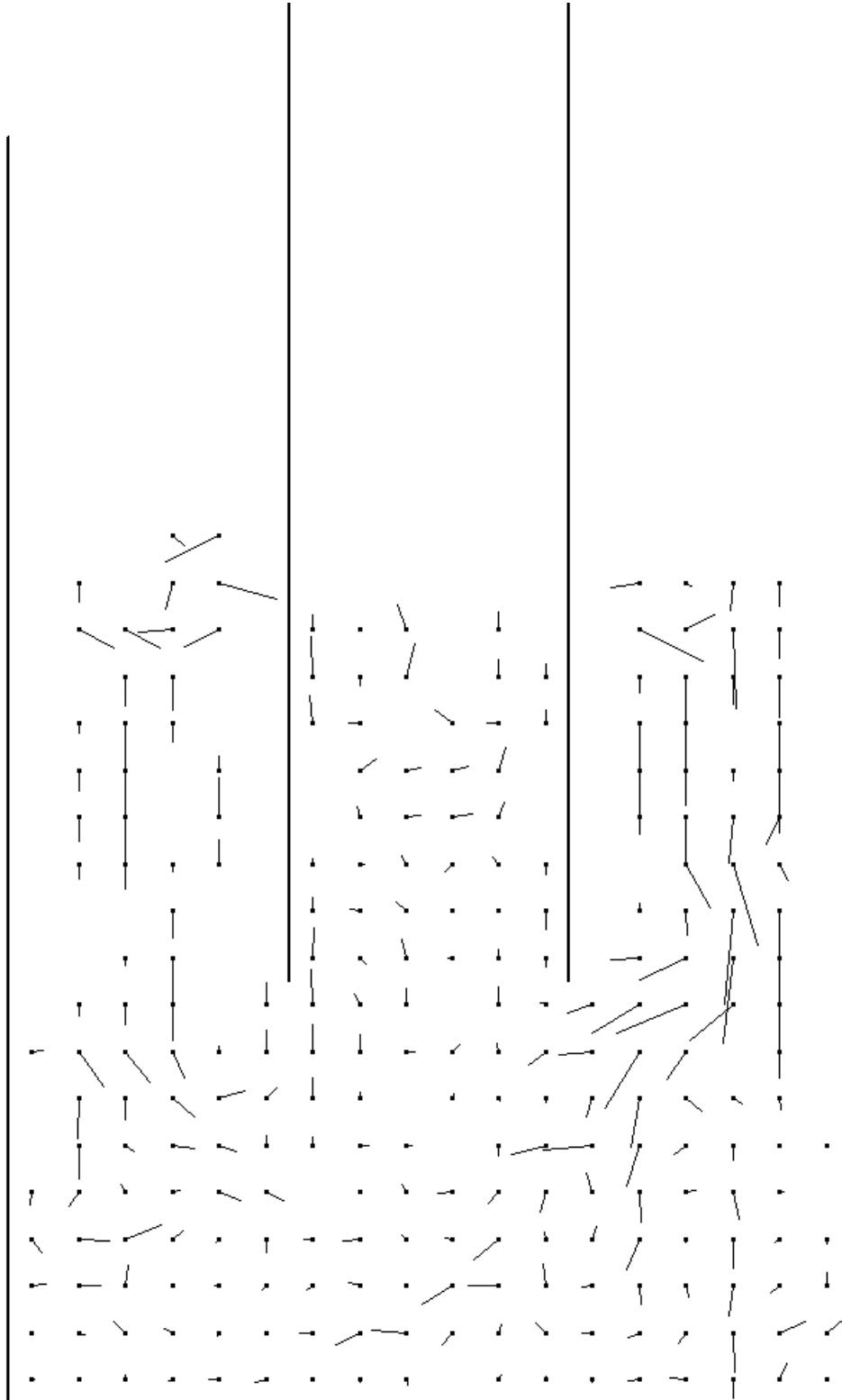


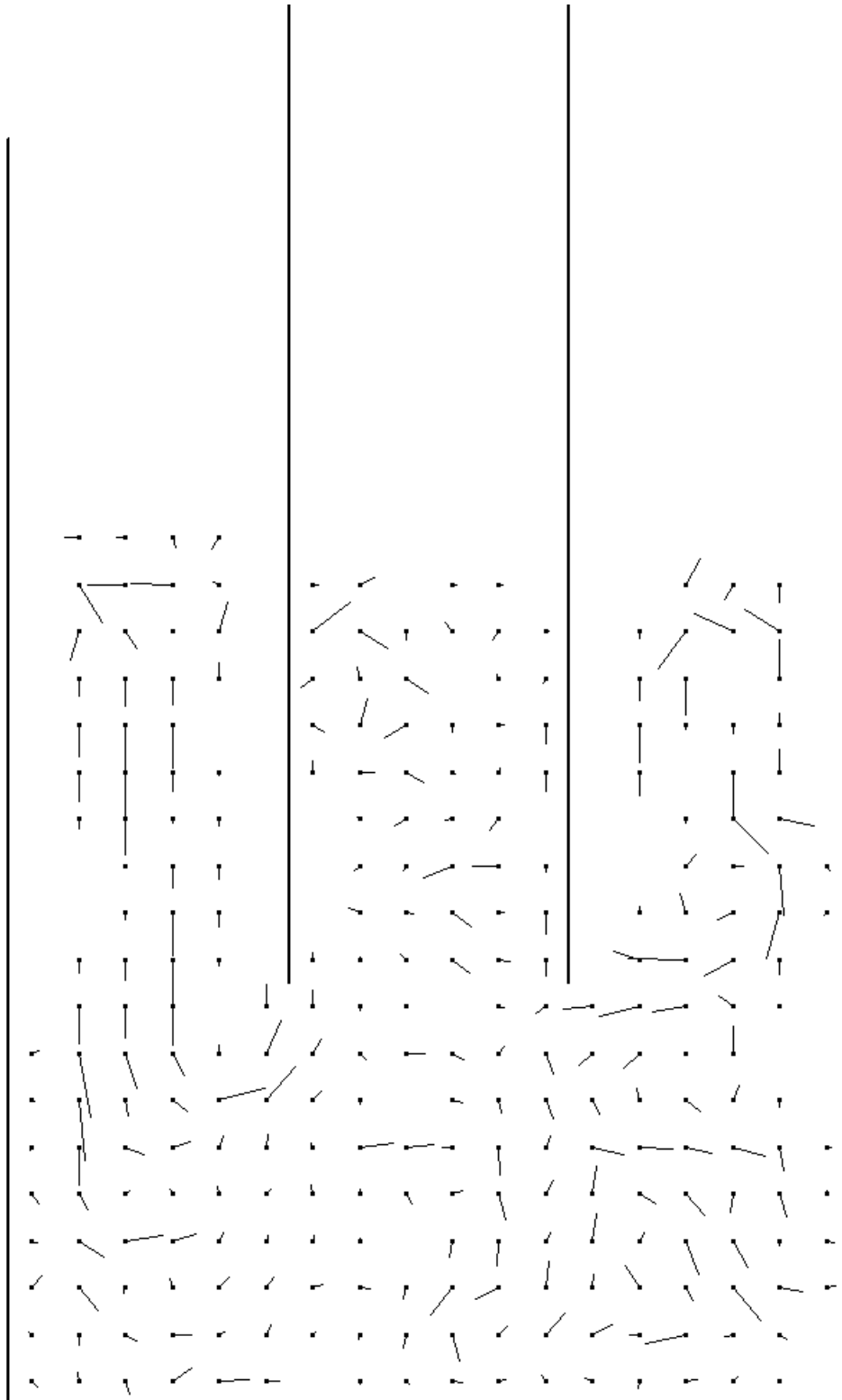
• • •

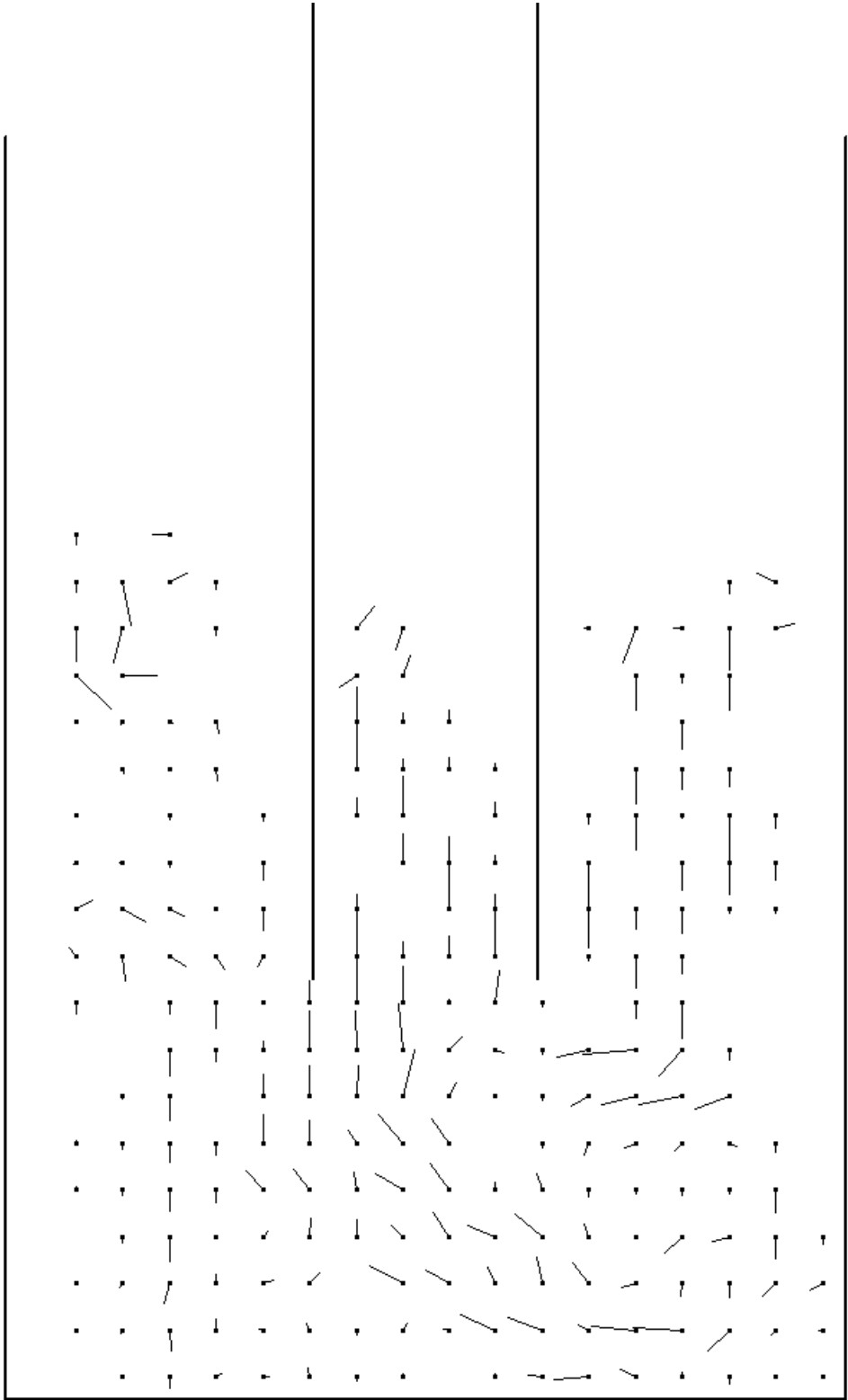


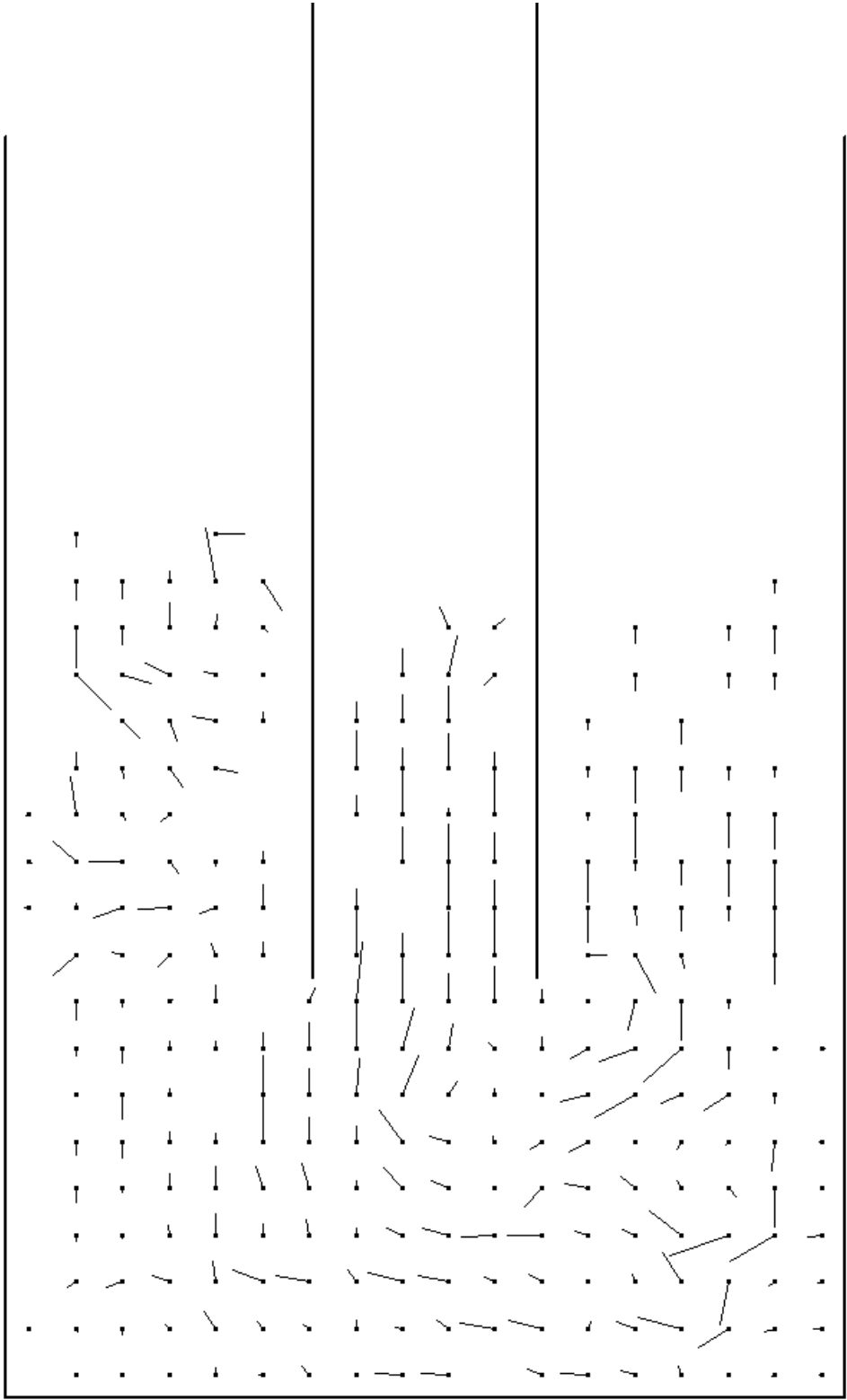


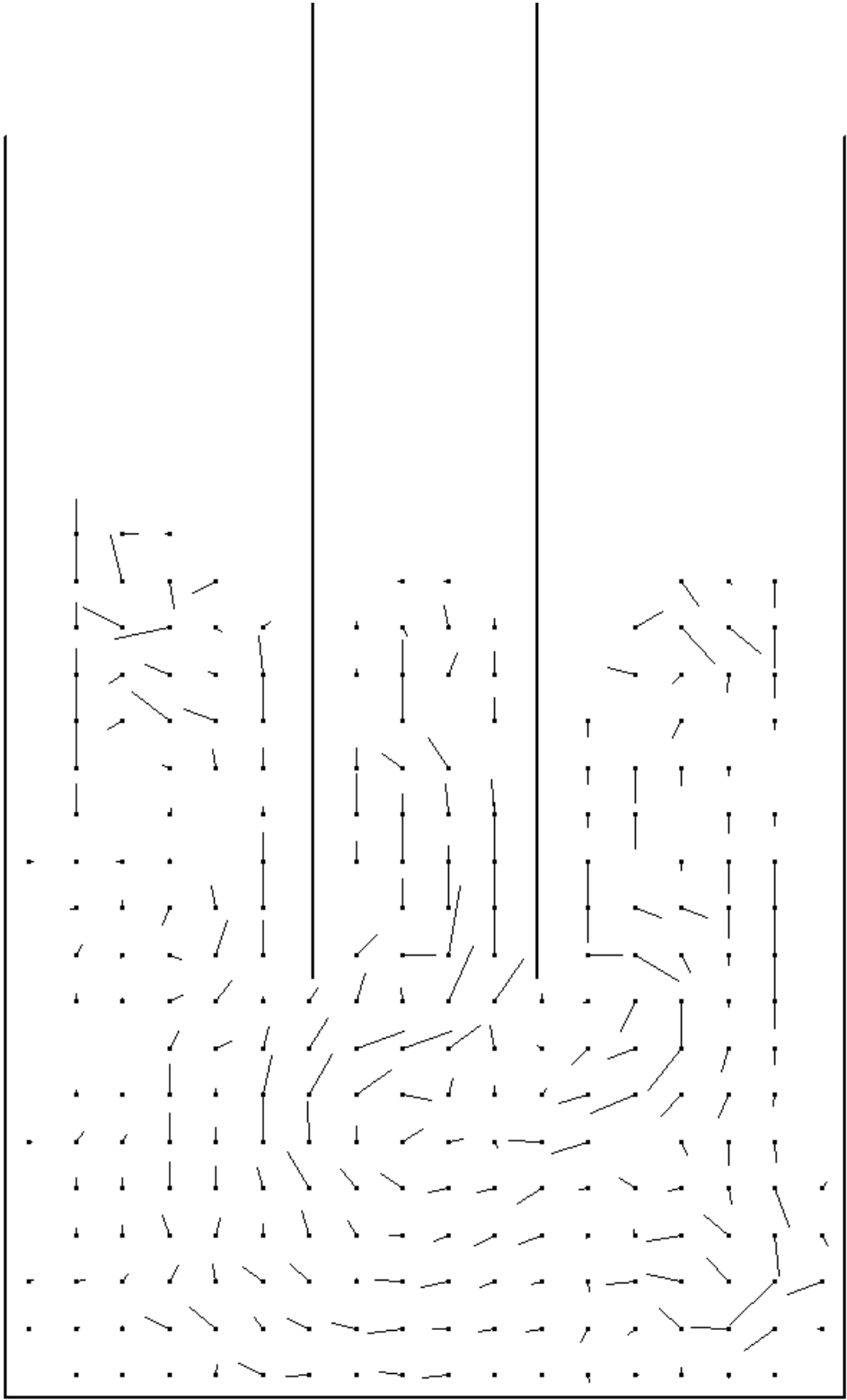


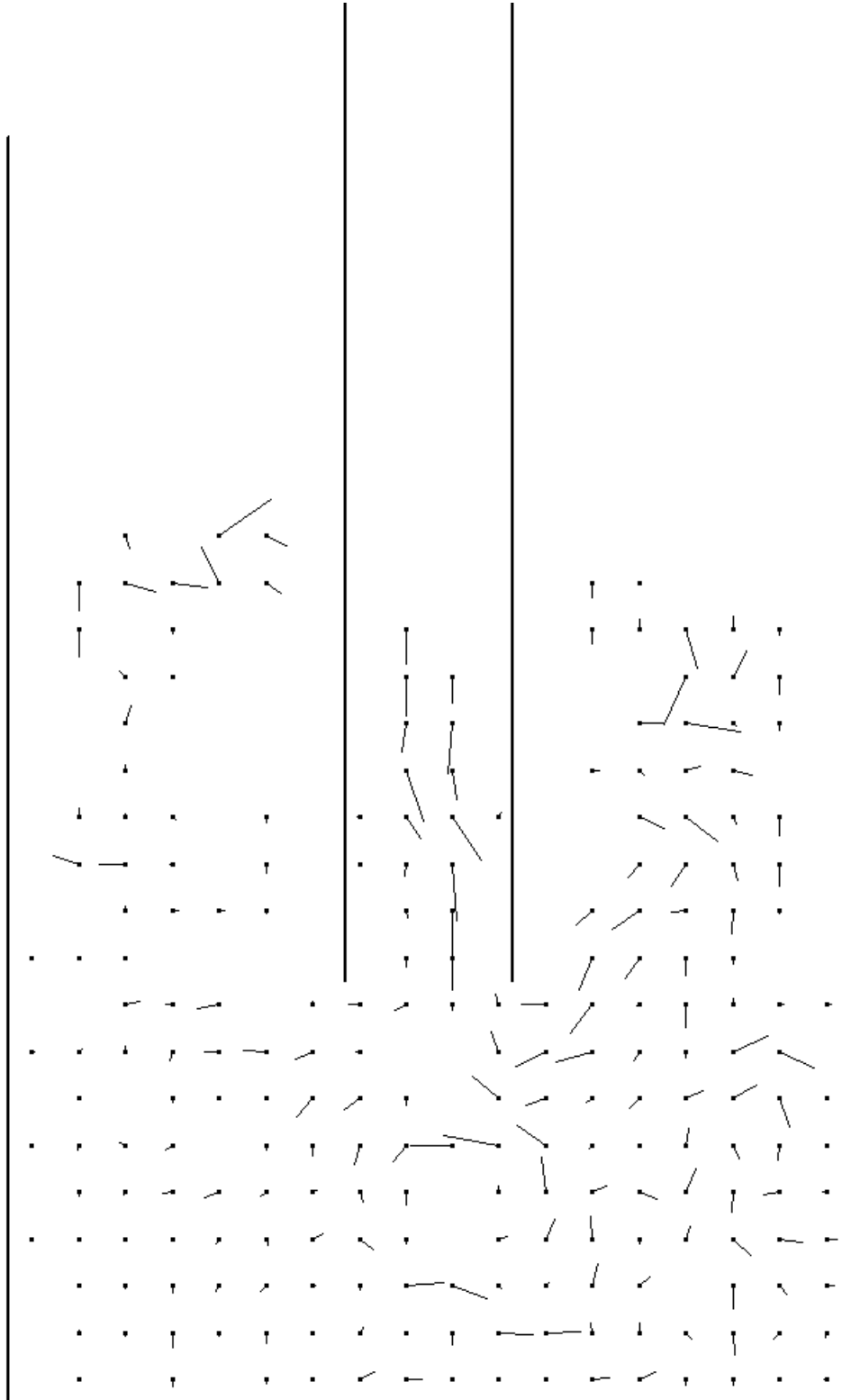


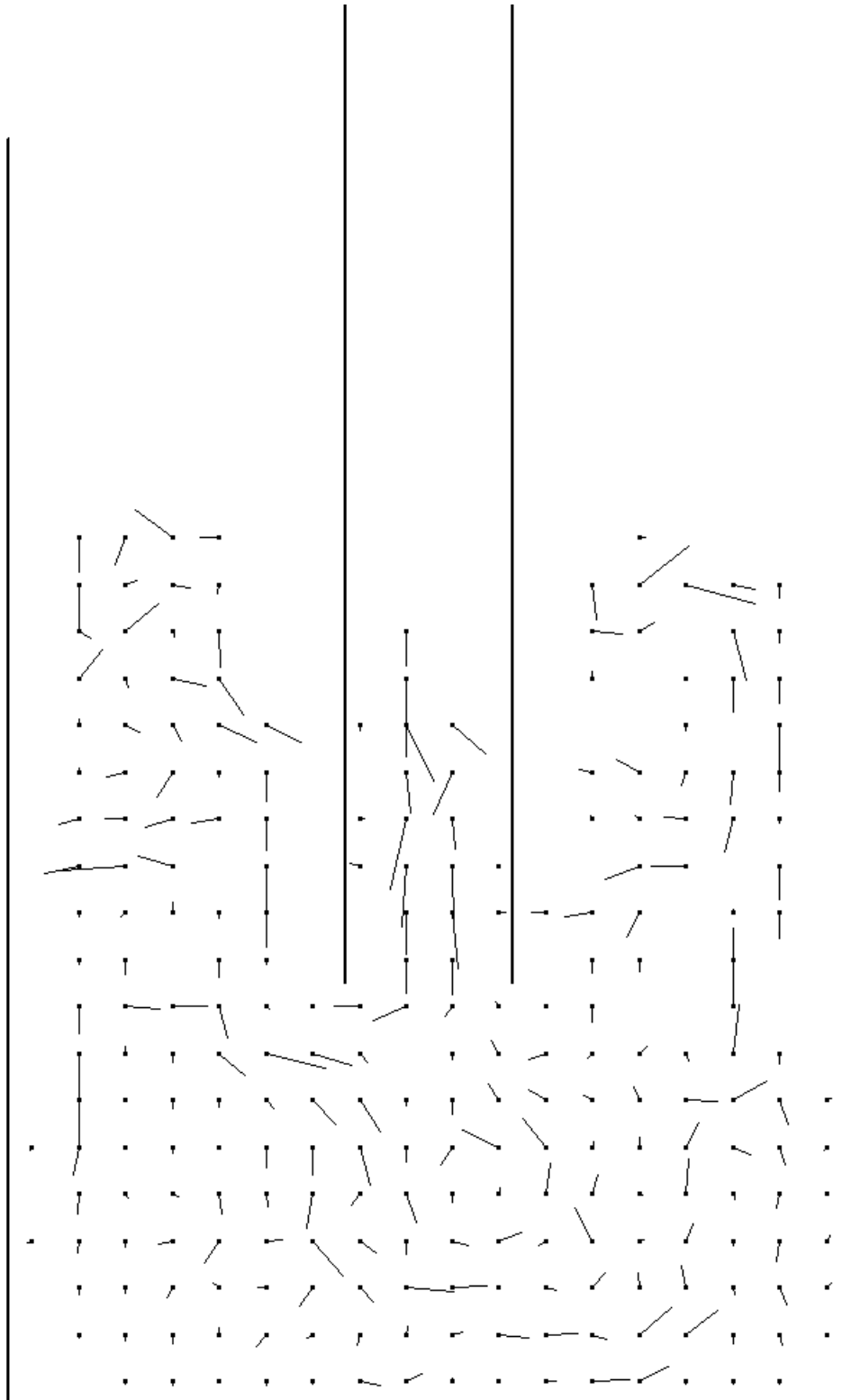


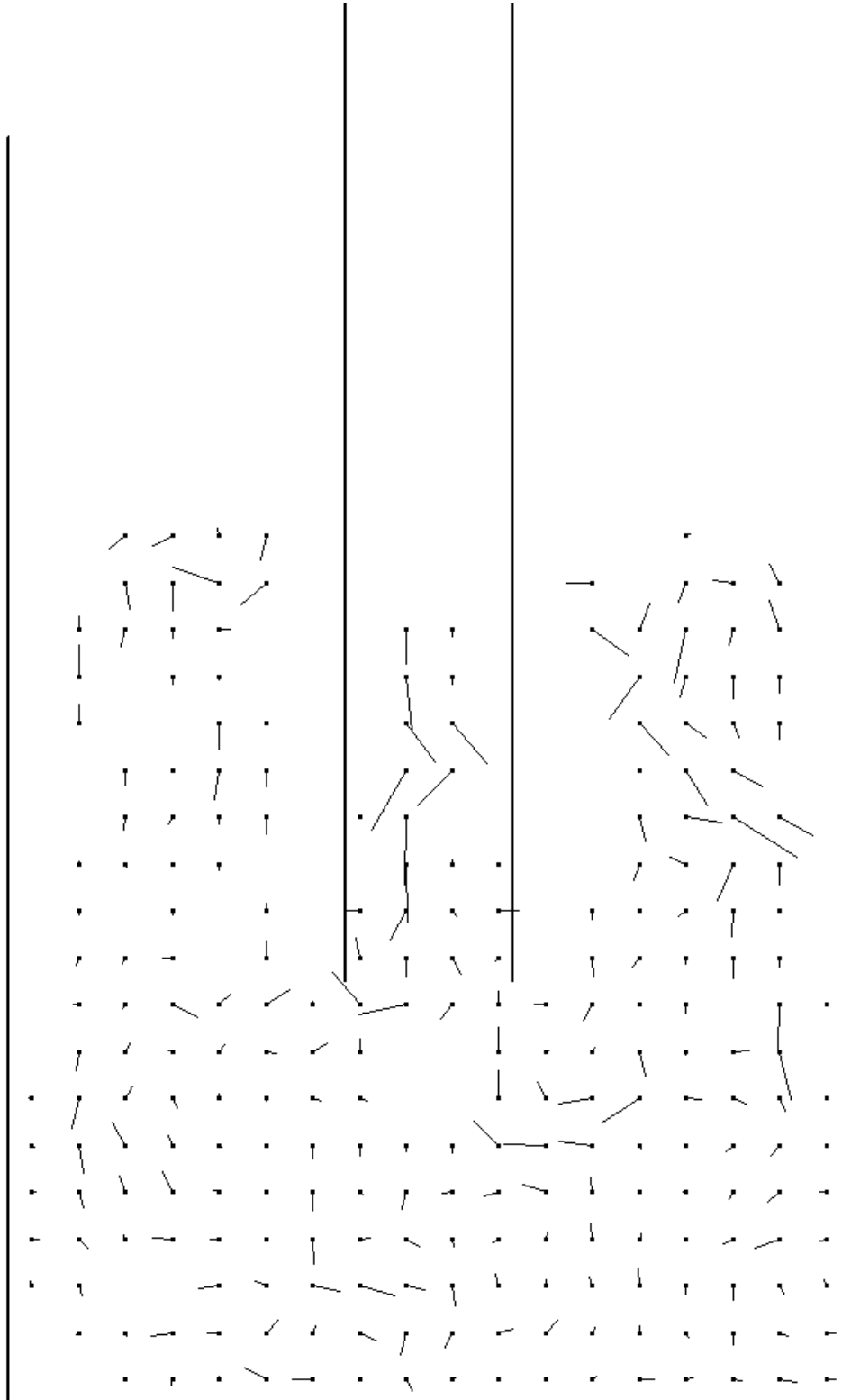


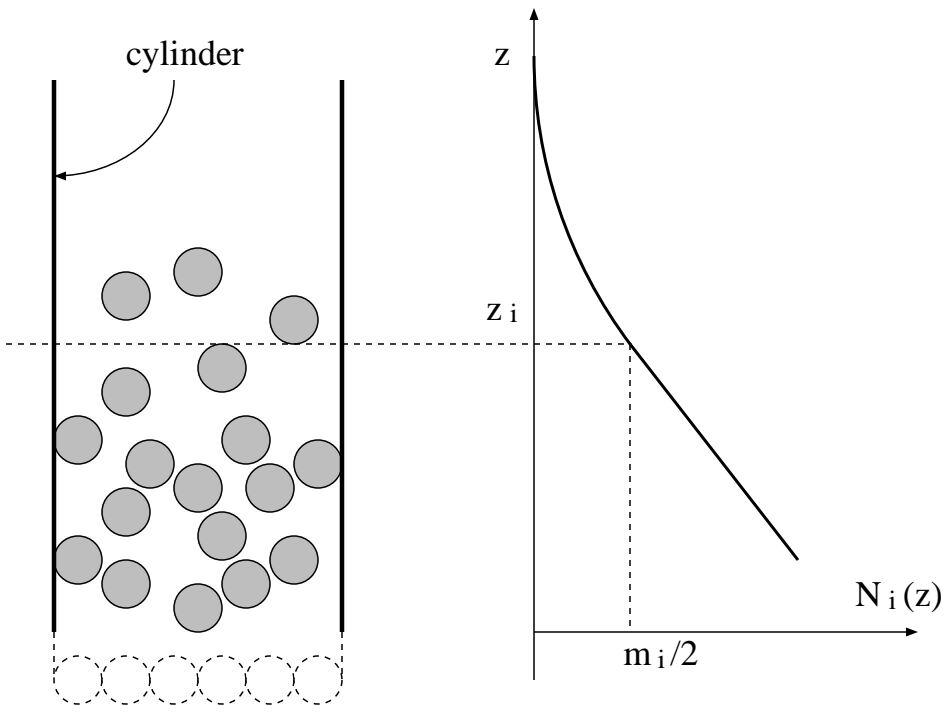


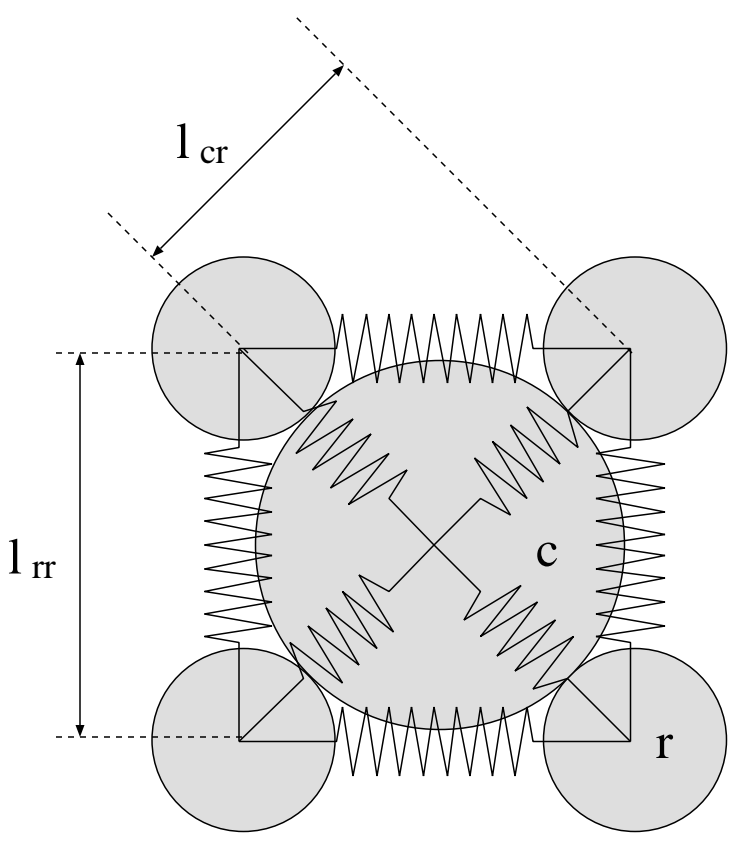




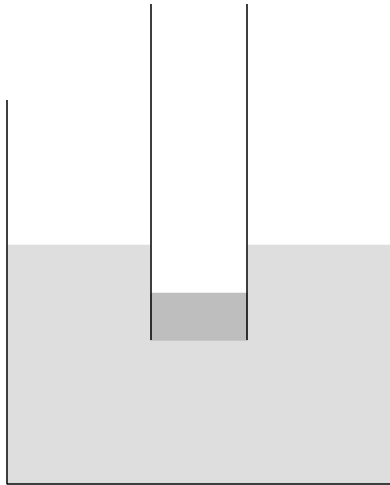




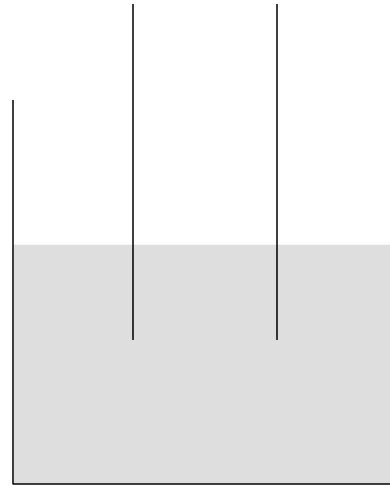




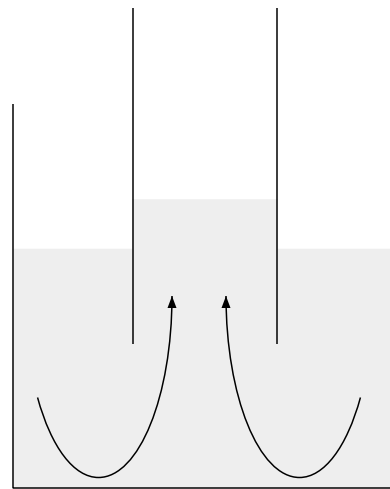
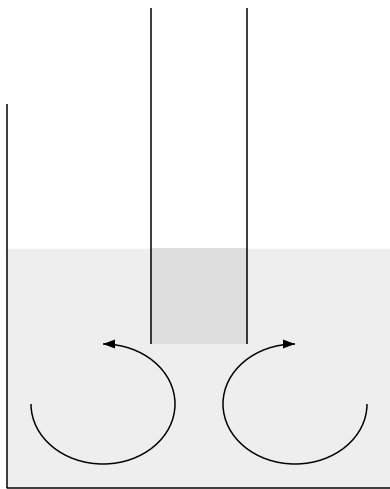
thin cylinder



thick cylinder



high angular velocity



low angular velocity

